NANO · MICRO small
www.small-journal.com

Recent Advances and Perspectives on the Polymer Electrolytes for Sodium/Potassium-Ion Batteries

Hang Yin, Chengjun Han, Qirong Liu, Fayu Wu,* Fan Zhang, and Yongbing Tang**

Owing to the low cost of sodium/potassium resources and similar electrochemical properties of Na^+/K^+ to Li^+, sodium-ion batteries (SIBs) and potassium-ion batteries (KIBs) are regarded as promising alternatives to lithium-ion batteries (LIBs) in large-scale energy storage field. However, traditional organic liquid electrolytes bestow SIBs/KIBs with serious safety concerns. In contrast, quasi-/solid-phase electrolytes including polymer electrolytes (PEs) and inorganic solid electrolytes (ISEs) show great superiority of high safety. However, the poor processibility and relatively low ionic conductivity of Na^+ and K^+ ions limit the further practical applications of ISEs. PEs combine some merits of both liquid-phase electrolytes and ISEs, and present great potentials in next-generation energy storage systems. Considerable efforts have been devoted to improving their overall properties. Nevertheless, there is still a lack of an in-depth and comprehensive review to get insights into mechanisms and corresponding design strategies of PEs. Herein, the advantages of different electrolytes, particularly PEs are first minutely reviewed, and the mechanism of PEs for Na^+/K^+ ion transfer is summarized. Then, representative researches and recent progresses of SIBs/KIBs based on PEs are presented. Finally, some suggestions and perspectives are put forward to provide some possible directions for the follow-up researches.

1. Introduction

In recent years, the demand for energy storage systems has been upsurging in many fields. Due to high voltage and energy density, good cycle stability, and less self-discharge performance, lithium-ion batteries (LIBs) have been widely used in various industries, such as portable electronic equipment and electric vehicles since the commercial LIBs were released for the first time in 1991.[1,2] Based on the Li metal anode, LIBs can reach a specific energy of 440 Wh Kg^{-1}, and further increase to 650/950 Wh Kg^{-1} for Li–S/Li–air battery systems, respectively.[3] However, environmental concerns and high-cost issues hinder the further commercial applications of LIBs, stemming from the low earth reserves and uneven distribution of the lithium resources (70% reserved in South America).[4–8] Compared with that in 1991, the cost of lithium resources has almost been double,[9,10] which goes against the development of the commercial applications. Besides, the insufficient abundance of lithium resources also poses a restriction to their potential application in large-scale energy storage fields.

One of the promising solutions is to develop sodium-ion batteries (SIBs)[11–17] and potassium-ion batteries (KIBs),[18–23] because of the high natural abundances (2.83 wt% for sodium and 2.59 wt% for potassium vs 0.002 wt% for lithium) and homogeneous distribution of sodium and potassium resources in the Earth's crust. **Table 1** shows the physical and chemical properties of Li, Na, and K elements. As seen, closely redox potentials of Na^+/Na and K^+/K (−2.71 V for Na^+/Na and −2.91 V for K^+/K versus standard hydrogen electrode (SHE)) to Li^+/Li (−3.04 V vs SHE),[24–26] smaller Stokes radius in propylene carbonate (PC) and water, and similar electrochemical activities of Na^+/K^+ ions bestow SIBs/KIBs with great potentials to sever as next-generation electrochemical energy storage systems for replacing LIBs.[9,27–39] In recent years, relevant works and reports on SIBs and KIBs have been exponentially increasing due to their appreciable application potentials in the large-scale energy storage field.[40–42] **Figure 1** statistically summarizes the yearly amounts of the reported scientific papers on SIBs (Figure 1a,c) and KIBs (Figure 1b,d) from 2010 to 2019,

H. Yin, Prof. F. Y. Wu, Prof. Y. B. Tang
School of Materials and Metallurgy
University of Science and Technology Liaoning
Liaoning, Anshan 114051, China
E-mail: fayuwu@ustl.edu.cn; tangyb@siat.ac.cn
H. Yin, C. J. Han, Dr. Q. R. Liu, Dr. F. Zhang, Prof. Y. B. Tang
Functional Thin Films Research Center
Shenzhen Institutes of Advanced Technology
Chinese Academy of Sciences
Shenzhen 518055, China
E-mail: qr.liu@siat.ac.cn
C. J. Han, Prof. Y. B. Tang
Nano Science and Technology Institute
University of Science and Technology of China
Suzhou 215123, China
Prof. Y. B. Tang
Key Laboratory of Advanced Materials Processing & Mold
Ministry of Education
Zhengzhou University
Zhengzhou 450002, China
The ORCID identification number(s) for the author(s) of this article can be found under https://doi.org/10.1002/smll.202006627.

DOI: 10.1002/smll.202006627

Table 1. The comparison between Li, Na, and K elements.[27,39,43]

Parameters	Li	Na	K
Relative atomic mass	6.94	23.00	39.10
Shannon's ionic radii [Å]	0.76	1.02	1.38
Stokes radius [Å] in PC	3.6	4.6	4.8
Stokes radius [Å] in water	1.25	1.84	2.38
Ionic volume [Å^3]	1.83	4.44	11.00
Density [g cm^{-3}]	0.534	0.97	0.862
Melting point [°C]	180.05	97.7	63.35
E° (vs SHE) [V]	−3.04	−2.71	−2.931
Theoretical capacity [mAh g^{-1}]	3861	1166	685
Theoretical capacity [mAh cm^{-3}]	2062	1131	591
Material abundance [ppm]	20	23 600	21 600
Distribution	70% in South America	Uniform	Uniform

respectively. As observed, in the past decade, the yearly number rapidly increases from several to hundreds, even thousands, suggesting that more and more efforts have been devoted to developing SIBs and KIBs.

In battery systems, electrolytes play a vital role in delivering the performance of batteries. For example, their coulombic efficiency of batteries closely relates to the electrochemical stability windows of electrolytes. Based on the molecular orbital theory, the highest occupied molecular orbital (HOMO)/lowest unoccupied molecular orbital (LUMO) energy correspond to the oxidative decomposition potential (ODP)/reductive decomposition potential (RDP), respectively.[44,45] When the ODP of cathode above the HOMO (or the RDP of anode below the LUMO) of electrolytes, some undesirable side reactions will occur at electrode/electrolyte interfaces such as electrolyte decomposition and formation of the passivation layer (**Figure 2**a).[46] To suppress these side reactions, the LUMO of electrolytes should be lower than the reduction energy of anode, as well as the HOMO of the electrolytes should be higher than the oxidation energy of the cathode,[26] which play a decisive role in the thermodynamic stability and voltage stable window of electrolytes.[47] A wider voltage stable window also

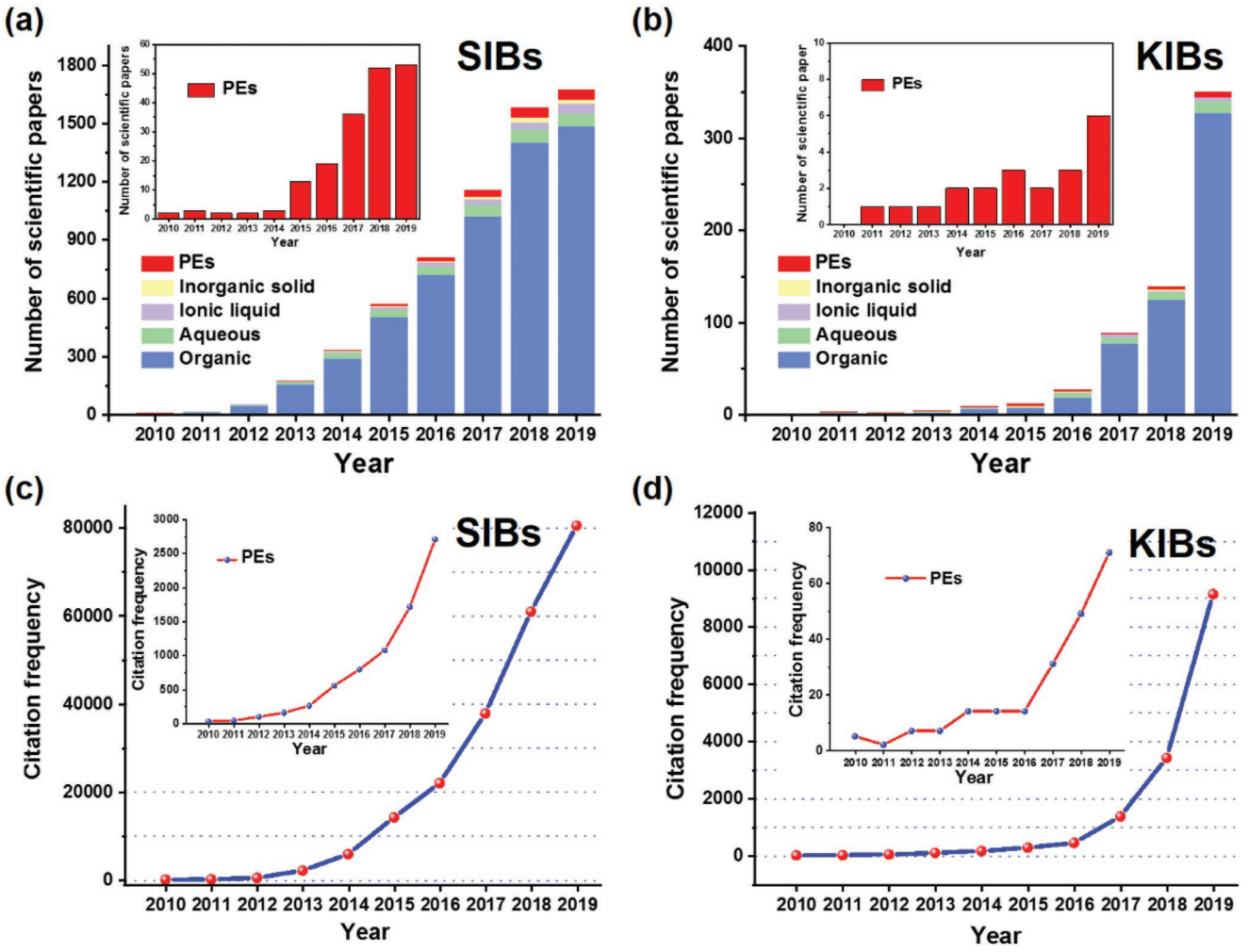

Figure 1. a,b) Yearly statistic amounts of the reported scientific papers on SIBs and KIBs, and c,d) their specific citation frequencies (from 2010 to 2019). Insets correspond to the relevant data of SIBs and KIBs based on polymer electrolytes (PEs), respectively. Note that the relative data are acquired from Web of Science.

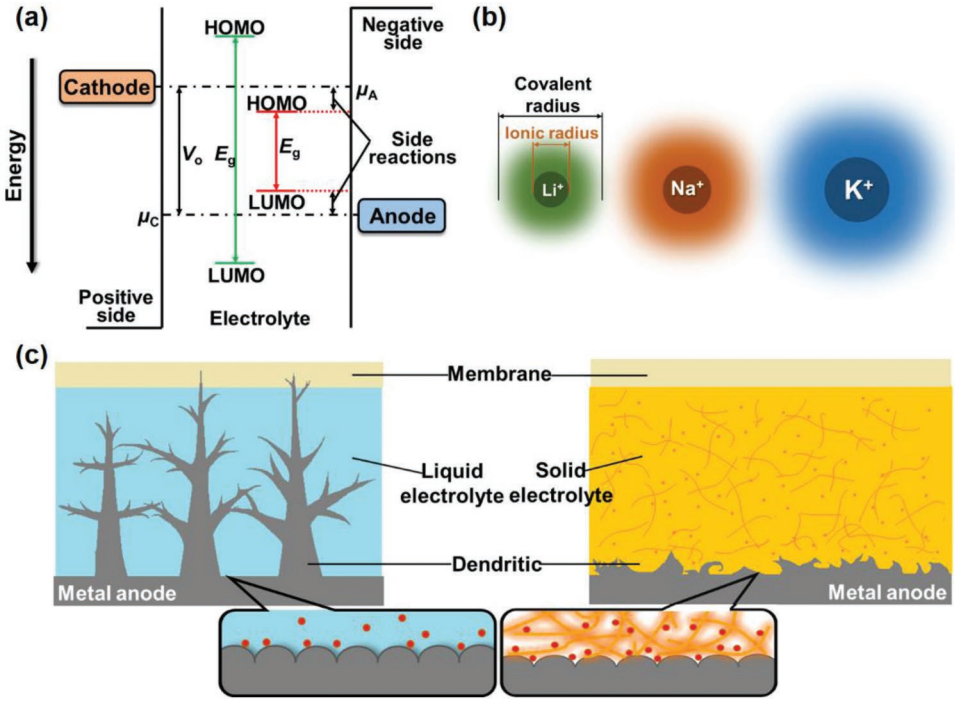

Figure 2. a) The HOMO/LUMO of the desired electrolyte (green) and unqualified electrolyte (red) and relate to the electrochemical potentials of the cathode (μ_c) and anode (μ_a). E_g and V_o represent the electrochemical window of electrolyte and open-circuit voltage of the battery, respectively. Adapted with permission.[46] Copyright 2010, American Chemical Society. b) Schematic covalent radius (halo part) and ionic radius (solid part). c) Dendritic growth in liquid (left) and solid (right) electrolyte, the electrode/electrolyte interface is amplified to observe interface contact.

means more choices in anode and cathode materials, allowing the batteries to deliver a higher operating voltage and therefore a higher energy density.

Besides, the solvation effect between solvent molecules and cation/anion is associated with the ionic kinetics and the stability of batteries. The intercalation/deintercalation and stripping/plating behaviors of active cations are always accompanied by the solvation/desolvation processes, which influence the kinetics of cations migration.[48,49] Figure 2b and **Table 2**[50] schematically show the covalent radius of Li^+, Na^+, K^+ and their corresponding desolvation energy in several typical organic solvents. On the one hand, a larger solvation structure may prevent cationic intercalation/deintercalation possess, thus results in kinetics retardation.[51] On the other hand, the desolvation energy represents the difficulty degree of solvation/desolvation processes. Furthermore, due to that solvation sheath molecules are supposed to be together with the cation diffusion, the solvent molecules may be first reduced by electrons and form the main ingredient of the solid electrolyte interphase (SEI).[52] The selection of solvent components plays a key role in the formation of SEI. Therefore, the solvation effect is directly related to the ionic transfer kinetics in batteries.

Further, the growth of dendrites and the flammability of electrolytes have raised serious safety concerns of batteries. A better fluidity of electrolytes enables faster transfer of ions and better interface infiltration as well,[53] which ensures the contact between electrode and electrolyte. In this regard, liquid-phase electrolytes show an obvious superiority over solid-phase electrolytes. When electrolyte changes from the liquid-phase to quasi-/solid phase, the interfacial contact becomes the main challenge; however, the enhanced mechanical strength and nonleakage nature is conducive to inhibiting the growth of dendrites and improving the safety (Figure 2c).[54,55]

Accordingly, it is of great significance to choose a suitable electrolyte for batteries. In consideration of the relatively high working voltage windows of SIBs and KIBs, one of the most widely used electrolytes is nonaqueous liquid electrolytes based on different organic solvents (PC, EC, EMC, DEC, dimethyl carbonate (DMC), dimethoxyethane (DME), etc.), electrolyte salts (sodium hexafluorophosphate ($NaPF_6$), potassium hexafluorophosphate (KPF_6), sodium bis(trifluoromethane) sulfonamide (NaTFSI), potassium bis(trifluoromethane)-sulfonimide (KTFSI), sodium perchlorate ($NaClO_4$), sodium bis(fluorosulfonyl)imide (NaFSI), potassium bis(fluorosulfonyl)imide (KFSI), etc.), and additives (FEC, VC, etc.).[56–59] In addition, aqueous liquid electrolytes (water as solvent), ionic liquid electrolytes, and quasi-/solid-phase electrolytes have also been attracting considerable attentions due to their high safety.[60,61]

Among these, the type of quasi-/solid-phase polymer electrolytes (PEs) has been attracted growing interest because PEs combine advantages of both liquid-phase electrolytes and inorganic solid electrolytes (ISEs).[26,62–66] Since Wright et al.[67] developed a PE composed of polyethylene (PEO) and alkali metal salt in 1973, substantial researches and efforts have been carried out toward high-performance PEs, which primarily focused on ion transfer mechanism, electrolyte/electrode interface, etc.[1,53,68–72] Up to now, various polymer matrix materials have been explored such as PEO, poly(vinylidene fluoride-hexafluoropropylene) (PVDF-HFP), poly(vinylpyrrolidone)

Table 2. Desolvation energy of Li^+, Na^+, and K^+ in common organic electrolyte solvents (data is derived from ref. [50]) (Note: EC denotes ethylene carbonate, EMC: methyl carbonate; DEC: diethyl carbonate; FEC: fluoroethylene carbonate; VC: vinylene carbonate).

Element	Desolvation energy [KJ mol^{-1}]					
	PC	EC	EMC	DEC	FEC	VC
Li	215.8	208.9	199.1	205.6	188.8	191.4
Na	158.2	152.8	143.1	147.9	136.2	138.3
K	119.2	114.6	101.6	105.1	100.5	102.2

(PVP), poly(vinyl alcohol) (PVA), etc. Although electrolytes using polymers as the host material are potential and advantageous, their properties remain to be improved, for example, ionic conductivity, cycling stability, etc. In the past decade, the yearly amounts of reported papers on PE-based SIBs and KIBs and corresponding specific citation frequencies were growing exponentially (insets in Figure 1).

Besides, Na/K metal anodes are capable of delivering high theoretical specific capacity and negligible volume changes accompanied by Na^+/K^+ plating/stripping during charge/discharge processes.[73] However, these metal anodes endow with high reactivity, which poses restriction on the development of Na/K metal anode-based SIBs and KIBs. Therefore, considering the inherent merits of PEs, combining PEs and sodium/potassium metal anodes is a promising path and maybe pave the way for next-generation energy storage systems. In this paper, we first discuss the advantages of different electrolytes and summarize the performance requirements for SIBs/KIBs. Then, representative researches and recent progresses of SIBs/KIBs based on PEs are presented. Finally, some suggestions and perspectives are put forward, hoping to be helpful for the follow-up researches.

2. Advantages and Ionic Migration Mechanism of PEs for SIBs/KIBs

As shown in Figure 1, great devotions have been made toward high-performance electrolytes for SIBs/KIBs in recent years.[53,63] Generally, the electrolyte community commonly includes five types of organic liquid electrolytes, aqueous electrolytes, ionic liquid electrolytes, ISEs, and PEs. Compared with others, each type presents some unique merits. **Figure 3** summarizes the critical performances of these electrolytes and makes comparisons among them.

Commonly, liquid-phase electrolytes endow with higher ionic conductivities (10^{-2} to 1 S cm^{-1}) than that of ISEs and PEs (10^{-7} to 10^{-3} S cm^{-1}) due to their good fluidity.[53] One of the most widely used electrolytes is organic liquid electrolytes. Once a suitable electrolyte has been designed, this type of electrolytes allows good electrochemical compatibility with electrode materials. However, their inherent flammability, ease leakage, and poor thermal stability give rise to serious safety concerns of combustion and explosion. In addition, possible side reactions and dendrite issues also pose challenges on the SIBs and KIBs based on organic liquid electrolytes. Particularly, in dual-ion battery (DIB) systems, high potentials (>4.5 V) of anion intercalation into graphite cathode generally result in the occurrence of severe side reactions.[71,74–77]

In contrast, aqueous electrolytes (water as solvent) and ionic liquid electrolytes show great safety superiority due to their natural nonflammability. Besides, aqueous electrolytes are favorable due to their environmental benignity and low cost. Nevertheless, the insufficient voltage window of aqueous electrolytes bestows aqueous SIBs and KIBs with low working voltages, and resultantly limited energy densities, even though "water-in-salt" strategy is able to obviously widen the electrochemical stability windows of aqueous electrolytes, allowing upper voltage of 2.5 V.[78–80] Besides, the dissolution of transition metal elements in aqueous electrolytes is also undesirable for improving the cycling performance of batteries. Differing from aqueous electrolytes, ionic liquid electrolytes are endued with strong tolerance to high voltage up to 5.0 V. Consequently, the application of ionic liquid electrolytes has attracted growing attention,[81] particularly in the DIB community. Unfortunately, their further application is restricted by the high cost, high viscosity, and insufficient compatibility with electrode materials.[82] More importantly, the dendrite growth and propagation are the main challenges facing Na/K-metal anode-based batteries with liquid-phase electrolytes (e.g., organic liquid electrolytes and ionic liquid electrolytes).[63,83]

It follows that these liquid-phase electrolytes individually show some intrinsic deficiencies and are incapable of satisfying the comprehensive requirements of high safety, wide

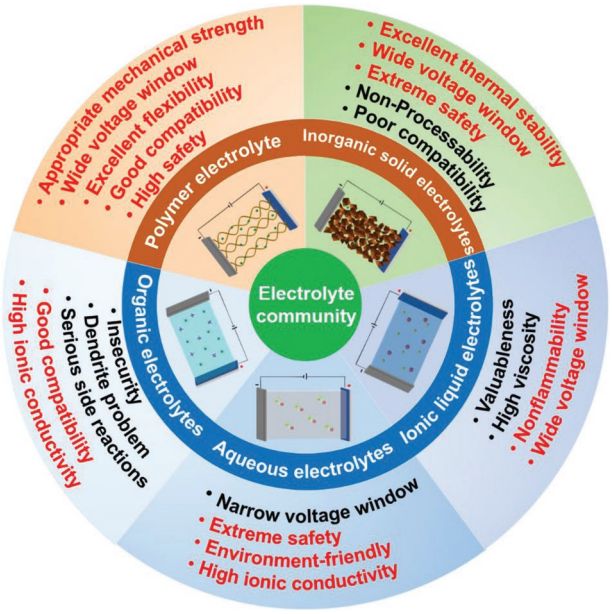

Figure 3. Comparison of merits and deficiencies among different electrolyte systems.

voltage stability windows, low cost, etc. Instead of these, quasi-/solid-phase electrolytes, including ISEs and PEs, have been being developed in recent years. Compared with liquid-phase electrolytes, the quasi-/solid-phase electrolytes take some great advantages of high safety, wide voltage window, and good thermal stability. 1) High safety: quasi-/solid-phase electrolytes can effectively prevent from the presence of liquid leakage and greatly improve the safety of batteries; 2) Wide voltage window: quasi-/solid-phase electrolytes are allowed to have enhanced electrochemical redox stability and resultantly to endow with a wide voltage window, which can readily match high-voltage cathode materials and provide feasibility for improving the energy density of batteries; 3) good thermal stability: quasi-/solid-phase electrolytes are capable of inhibiting the accident induced by thermal runaway. However, for ISEs, the main challenges are their low ionic conductivity originating from the sluggish kinetics of Na^+ ions and K^+ ions, and poor interfacial contact between electrolyte and electrodes.[84] Although sulfide ISEs have been reported to present high ionic conductivity for Na^+ ions,[85,86] their vulnerability to ambient atmosphere poses restriction to the practical application. Meanwhile, ISEs also endow with a poor large-scale processibility due to their natural brittleness.[62,87,88]

Compared with liquid-phase electrolytes and ISEs, PEs also show other comprehensive superiorities. For example i) appropriate mechanical strength of PEs enables the uniform plating/stripping of active alkali metal ions on the surface of anode and resultantly suppresses the formation and growth of dendrites. And ii) excellent flexibility, different from the natural brittleness of ISEs, bestows PEs with great potential in the field of wearable energy-storage devices. It is also noteworthy that, compared with ISEs, PEs can effectively accommodate volume changes of electrode materials during the charging/discharging processes without compromising interfacial contact.[89] iii) Good processibility and facile/scalable preparation processes,[90] particularly for in situ polymerized PEs, enable great processing compatibility with the existing preparation procedures of batteries based on liquid-phase electrolytes.[91] Furthermore, iv) PEs take advantage of good interfacial contact and electrochemical compatibility over ISEs because the natural rigidity of the latter generally results in the presence of interfacial gaps and resultantly poor interfacial contact between electrolyte and electrodes. v) PEs are more conducive to realizing high ionic conductivity for the transfer of Na^+ ions and K^+ ions at room temperature or even at low temperature than ISEs, due to the large ionic radii of active ions and different ion migration mechanism between PEs and ISEs.[92] vi) PEs also have some other merits of lightweight, high-volume utilization, and good film-forming ability.[90]

To further improve the electrochemical properties of PEs, it is of significance to get fundamental insight into the migration mechanism and transfer kinetics of active ions in PEs. It is generally accepted that the Li^+-ion migration in PEs is affected by the fracture/formation of coordination bonds in the segmented movement of polymer chains, which mainly occurs in the amorphous region of the polymer matrices.[93] For example, Li^+ ions first locate at the active site provided by the polar group of PEs (e.g., −O− in PEO). Under the driving of the electric field, the local segmental motion of polymer chains induces Li^+ ions to move/leap from one coordination site to another adjacent active site, and thus realizes ion migration.[62] It is theoretically reasonable to infer that the migration of Na^+/K^+ ions in PEs shares a similar mechanism with that of Li^+ ions, since Na^+/K^+ ions have similar electrochemical activity with Li^+ ions. However, it is noteworthy that the migration process of different active ions in PEs is not only associated with the type of active ions (ionic radius, charge density, etc.) and inactive ions (bonds with polymer matrix), but also involves the dielectric constant, amorphous phase characteristics, mobility of the polymer matrix, etc.[91]

Figure 4 summarizes the merits and deficiencies of several typical PE matrices. Poly(ethylene oxide) (PEO), one of the most typical polymers for PEs, has a repeating $-CH_2CH_2O-$ (EO) group with lone pair electrons that can be attached by metal ions. The PEO-based electrolytes show excellent salt dissociation ability and good mechanical strength and advantages of being relatively cheap and not susceptible to moisture. However, the low ionic conductivity induced by the high crystallinity and narrow electrochemical window at room temperature limits their development.[94,95] Poly(vinylidene fluoride-hexafluoropropylene) (PVDF-HFP), consisting of a crystalline phase (-VDF) for mechanical enhancement and an amorphous phase (-HFP) for reducing the degree of crystallinity, exhibits a high dielectric constant (ε = 8.4), outstanding mechanical strength, excellent electrochemical stability, and thermal stability, and is one of the most commonly used PE matrices.[96] Due to extremely low glass transition temperature of polyphosphazenes (PAN), PAN-based electrolytes are conducive to improving ionic conductance, and have excellent oxidation resistance and thermal stability.[97] However, their mechanical strength and reduction-resistive ability are not sufficient, and their synthesis route is relatively complex. The rich ester group in poly(methylmethacrylate) (PMMA) has a strong interaction with the oxygen atoms in the carbonate plasticizer, resulting in its strong ability to dissolve massive liquid electrolytes.[98] Therefore, the PMMA-based PEs generally have a high ionic conductivity. The presence of a large number of side-chain carbonyl groups in polyvinyl pyrrolidone (PVP) endows with excellent dissociation ability and a high amorphous region, allowing faster ion migration.[37] In addition, PVP can provide excellent thermal stability and mechanical strength for blended materials. Relatively cheap poly(vinyl chloride) (PVC) also contains rich C−Cl bond, which makes it have a strong binding ability with electrolyte salts, and is compatible with a large number of plasticizers. Therefore, the rational design of PEs should fully take into consideration the components of PE matrices and the type of electrolyte salts. In the next two sections, the advance of PEs for SIBs and KIBs will be summarized and reviewed in detail.

3. PEs for Na-Ion Batteries

3.1. Solid PEs (SPEs)

3.1.1. PEO-Based SPEs

PEO matrix is widely used in SPEs due to their high solvating power with alkali metal ions, good processability, and

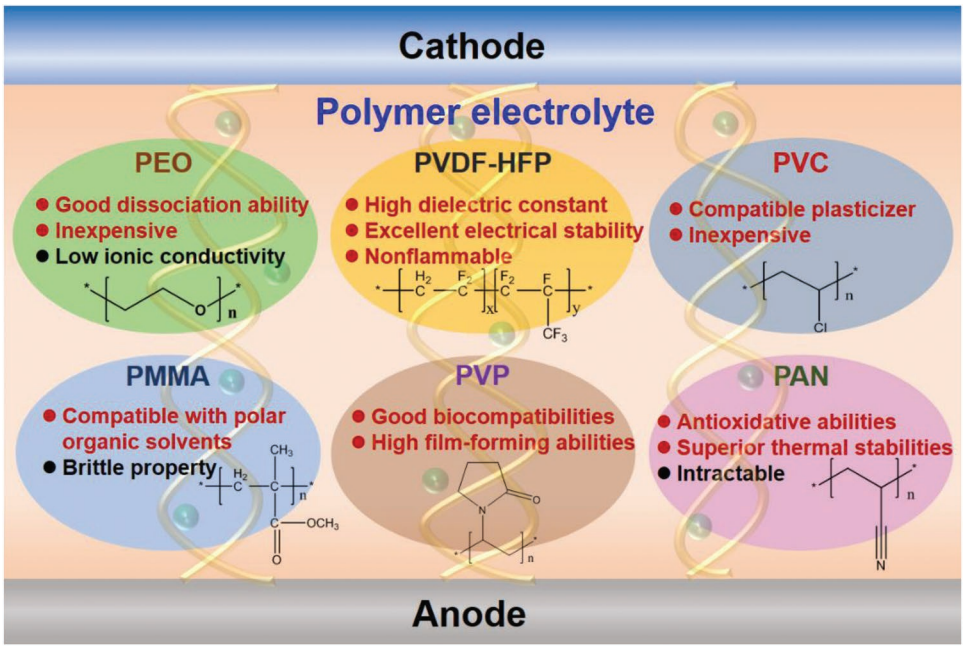

Figure 4. Several typical PE matrices and their individual advantages and demerits.

mechanical properties.[99] It has been demonstrated that ion migration in PEs is mainly carried out via the amorphous rather than crystalline regions. As a semicrystalline polymer, amorphous and crystalline phases coexist in PEO, which has been considered as one of the main reasons for low ionic conductivity of PEs.[100,101] Many efforts have been devoted to limiting the crystallization level of PEO-based electrolytes, for example, the addition of nanofillers, blending polymers, screening of Na-salts, etc., and thus to increasing the amorphous phase and improving the ionic conductivity of PEO-based SPEs.

Inorganic nanoparticles are widely used as nanofillers in PEs, which presents superiority in improving ionic conductivity over that without adding inorganic nanofillers.[94,102] The improved effect can be ascribed to that nanoparticles form an associated network in the polymer and breach the ordered structure of PEO, which is conducive not only to improving the ionic conductivity but also to boosting their mechanical strength. There are many compatible inorganic nanofillers such as TiO_2, Al_2O_3, SiO_2, $BaTiO_3$, CuO, ZrO_2, etc.[103–110] Ni'mah et al.[100] reported a SPE of PEO/TiO_2/$NaClO_4$ (TiO_2 = 3.4 nm, 5 wt%), in which the ratio EO:Na (denoting the degree of Na^+ ion solvation by PEO oxygen atoms) was 20:1. The addition of TiO_2 nanofillers could effectively restrain the recrystallization of PEO, so that boost the formation of amorphous phases and promote ionic transfer as well (**Figure 5**a). As a result, such the electrolyte presented an enhanced ionic conductivity of 2.62×10^{-4} S cm^{-1} at 60 °C. Assembled $Na_{2/3}Co_{2/3}Mn_{1/3}O_2$ cathode with Na metal anode, the obtained battery with the PE delivered a discharge capacity of 49.2 mAh g^{-1} at 0.1 C with 91.5% capacity retention after 25 cycles. Further, Arya et al.[111] comparatively studied the effect of different shapes of TiO_2 nanoparticles (nanofiller vs nanorod) on electrochemical properties of SPEs, and showed that the ionic conductivity was sensitive to the shape of nanoparticles, and the PE with the addition of TiO_2 nanorods presented superior properties (dielectric nature, electrochemical window, ionic conductivity) than that added with TiO_2 nanofillers.

NASICON-type ISE materials can also be applied as the fillers.[112] On the one hand, the addition of NASICON-based fillers is beneficial to promote the amorphization of PEO, and on the other hand, can serve as the high-speed ionic channels for Na^+ ions transfer. Yu et al.[113] added $Na_3Zr_2Si_2PO_{12}$ into PEO polymer, and the obtained SPE (PEO/25 wt% $Na_3Zr_2Si_2PO_{12}$/$NaClO_4$) delivered a high ionic conductivity of 5.6×10^{-4} S cm^{-1} at 60 °C. Similarly, Zhang et al.[87] introduced $Na_{3.4}Zr_{1.8}Mg_{0.2}Si_2PO_{12}$ nanoparticles into PEO-based SPE, which greatly enhanced the ionic conductivity up to 2.4×10^{-3} S cm^{-1} at 80 °C.

Besides, previously reported studies on the transfer kinetics of Li^+ ions in PEs have shown that the smaller particle size of nanofillers is beneficial to allow faster transfer kinetics of cations.[87] However, the agglomeration of nanoscale oxides quickly takes place to form larger particles. In order to avoid the agglomeration, Wei's group[114] reported a carbon quantum dots (CQDs, 2.0–3.0 nm) with high dispersion by a simple synthesis method (the synthesis mechanism was schematically shown in Figure 5b), and the addition of the CQDs endowed the PEO-based SPE with an ionic conductivity of 7.2×10^{-5} S cm^{-1} at ambient temperature. Such enhanced effect could be explained by that introducing smaller and more dispersed CQDs enhanced the dissociation of Na-salts, so that the crystal size of polymer was reduced and accompanied by the expanded amorphous region (Figure 5b). Consequently, the assembled battery with the configuration of $Na_3V_2(PO_4)_3$‖PEO/CQDs-Na‖Na exhibited an initial discharge capacity of 101.5 mAh g^{-1} at 1 C and a capacity retention of 88% after 100 cycles. **Table 3** shows the specific performance of PEO-based SPEs with the addition of different nanoparticles.

Each PE matrix features their superiorities and demerits. The composite design of two or multiple components is beneficial

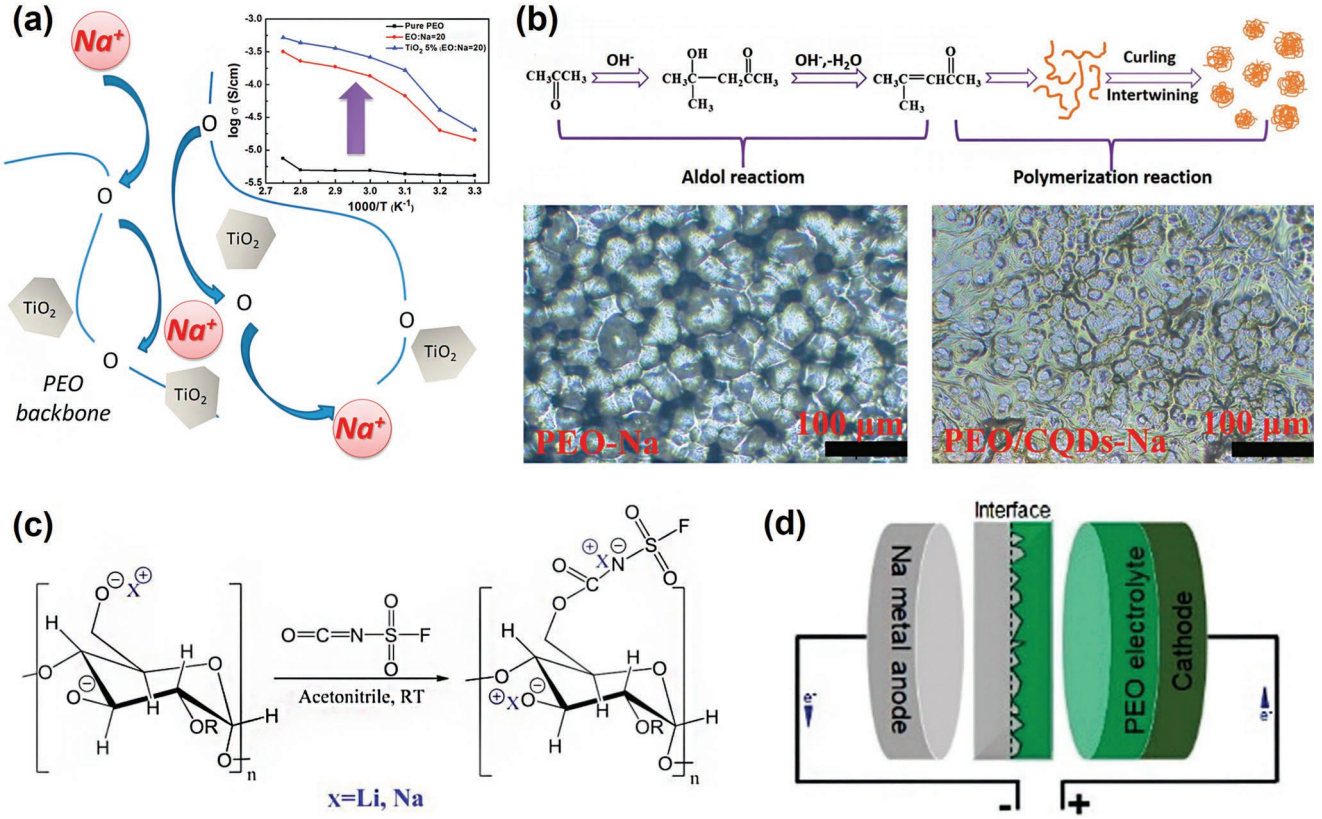

Figure 5. a) Illustration of TiO_2 nanoparticles doped into PEO backbone. Reproduced with permission.[100] Copyright 2015, Elsevier. b) Schematic illustration of the synthesis mechanism for CQDs and polarized light microscopy of PEO-Na and (left) PEO/CQDs-Na (right). Reproduced with permission.[114] Copyright 2018, Wiley-VCH. c) The synthesis schematic of Na(FSI-ethylcellulose); Reproduced with permission.[121] Copyright 2020, Elsevier. d) Illustration of the interfacial phase for solid-state polymer Na-metal batteries. The synthesis schematic of Na(FSI-ethylcellulose). Reproduced with permission,[124] Copyright 2019, Wiley-VCH.

to combine their advantages. Designing a mixture PE matrix of PEO with other polymers is also a feasible way to improve ionic conductivities for PEO-based PEs. Kumar et al.[101] reported the first PEO/PVP mixture system for Na^+-ion SPEs with an ionic conductivity of 1.19×10^{-7} S cm^{-1}. Compared to semicrystal PEO, the PVP polymer endows with more amorphous regions. Besides, the functional carbonyl groups (C=O) in PVP enable to combine with a variety of Na-salts ($NaPF_6$, NaF, NaBr, $NaIO_4$, etc.).[87,101,115–117] Recently, Pritam et al.[118] designed a composite SPE with a composition of PEO/PVP/$NaNO_3$ (EO:Na = 14) that delivered an ionic conductivity of 2.92×10^{-5} S cm^{-1} at ambient temperature. The study also suggested that increasing the concentration of Na-salts was helpful for elevating the number of carriers as well as conductivity in a certain concentration range.

Some issues such as concentration polarization and decomposition always exist in SPEs. One of the solutions is to restrict the mobility of anions by bonding them with polymer chains and simultaneously to obtain high mobility of cations, which is also beneficial to prevent electrolytes from the consumption.[119,120] Youcef et al.[121] developed a single ion conductive system of PEO/NaFSI/ethyl-carboxymethyl cellulose by a single synthesis method, which could be carried out with economic benefits and environmental friendliness. Functionalizing ethylcellulose with anions in NaFSI formed a Na–salt complex of

Table 3. Electrochemical performance of PEO-based SPEs with different inorganic nano-fillers and corresponding batteries.

Electrolyte composition	Ionic conductivity [S cm^{-1}]	Voltage window	Battery configuration	Capacity [mAh g^{-1}]
PEO/NaTFSI/SiO_2[122]	1.1×10^{-3} at 80 °C	4.2 V	Super P/Na	
PEO/TiO_2/$NaClO_4$[100]	2.6×10^{-4} at 60 °C	4.3 V	$Na_{2/3}Co_{2/3}Mn_{1/3}O_2$/Na	49.2 at 0.1 C
PEO/$Na_{3.4}Zr_{1.8}Mg_{0.2}Si_2PO_{12}$/NaFSI[87]	2.4×10^{-3} at 80 °C	4.37 V	$Na_3V_2(PO_4)_3$/Na	106.1 at 0.1 C
PEO/Na[$(FSO_2)(n\text{-}C_4F_9SO_2)N$][123]	3.4×10^{-4} at 80 °C	4.87 V	$NaCu_{1/9}Ni_{2/9}Fe_{1/3}Mn_{1/3}O_2$/Na	122.4 at 0.1 C
PEO/CQDs/$NaClO_4$[114]	7.17×10^{-5}	4.5 V	$Na_3V_2(PO_4)_3$/Na	101.5 at 1 C
PEO/PVP/$NaNO_3$[118]	2.92×10^{-5}	≈4 V	–	–
PEO/Na(FSI-ethylcellulose)[121]	7.6×10^{-5} at 70 °C	4.3 V	C/Na	220 at 0.05 C

Na(FSI-ethylcellulose) (Figure 5c), boosting an enhanced ionic conductivity of 7.6×10^{-5} S cm^{-1} and a Na^+-ion transference number of 0.6.

Compare to the liquid-phase electrolytes with excellent wettability, solid-phase electrolytes generally suffer from fewer contact sites and higher interface resistance because of their poor fluidity along with an insufficient contact area between electrodes and electrolyte. And, the issue of interfacial compatibility between electrodes and electrolyte also results in sluggish kinetics of Na^+ transport. Therefore, improving the electrodes/electrolyte interfacial contact is of great significance for enhancing the rate performance as well as the cycle stability of solid-state batteries. A typical PE was composed of PEO matrix and NaFSI salt (PEO_{20}NaFSI) with a molar ratio of 20 (EO/Na^+). However, when the PE was paired with pure Na metal anode to form Na‖PEO_{20}NaFSI‖Na symmetric cells, the electrochemical polarization for Na plating/stripping was obviously enlarged after some cycles.[71,90] Accordingly, in order to improve the interfacial compatibility between the PE and Na metal anode, Zhao et al.[124] introduced a carbon matrix into the Na metal anode to construct a Na/C composite anode (Figure 5d). On the one hand, the carbon material was stable toward Na metal anode with high reactivity and had a strong bond with Na metal. Besides, the ionic and electronic conductivities of the carbon were conducive to boosting the Na plating/stripping. On the other hand, the carbon material was likely to form strong covalent bonds with PEO due to their possible reactions between them and to prevent the PE from the delamination, and thus to enhance the interfacial connectivity between SPE and the Na metal anodes. Additionally, the carbon matrix with a 3D structure would effectively distribute Na plating/stripping onto a large surface area and reduce the local current density on the composite anode, and hence was expected to enhance the cycling reversibility.[125] Such a modification bestowed the Na/C‖PEO_{20}NaFSI‖Na/C symmetric cell with a lower electrochemical overpotential of ±80 mV at 0.6 mA, and enhanced cycling stability up to 800 h at 0.3 mA (tested at 80 °C). In contrast, a short circuit was presented after 138 cycles for Na‖PEO_{20}NaFSI‖Na. A full cell with a configuration of Na/C‖PEO_{20}NaFSI‖$Na_3V_2(PO_4)_3$ was assembled to study the effect of the interfacial modification. As a result, the full cell delivered a higher reversible capacity of ≈111 mAh g^{-1} and smaller electrochemical overpotential of ≈36 mA at 0.1 C (vs 102 mAh g^{-1} and 60 mV, respectively, for Na‖PEO_{20}NaFSI‖$Na_3V_2(PO_4)_3$). Besides, with a modified Na/C anode, the full cell presented a reinforced cycle performance (capacity retention above 92%, 80%, 70% after 2000, 5000, 8000 cycles, respectively).[90]

3.1.2. Non-PEO-Based SPEs

As mentioned above, although PEO-based SPEs are widely investigated due to some merits of good processibility, superior electrochemical stability, etc., their further development is restricted by their low ionic conductivities (10^{-7}–10^{-8} S cm^{-1} at room temperature and 10^{-4}–10^{-5} S cm^{-1} at 60 °C) because the high crystallinity of PEO at room temperature is harmful to the migration of active cations.[126] The corresponding solid-state SIBs have to be operated at elevated temperatures. However, the high reactive ability and the low melting point of Na metal give impetus to developing room-temperature or low-temperature solid-state SIBs.

Accordingly, some efforts have gradually been diverted to non-PEO-based PE systems. Du et al.[127] designed a novel polymer-based SPE (PFSA-Na-SPE) of PFSA-Na/$NaClO_4$/EC/DEC (PFSA-Na denotes a perfluorinated sulfonic resin powder in the Na-form) by a facile large-scale ionic-exchange strategy (**Figure 6**a). The obtained SPE not only presented excellent mechanical properties, enabling the suppression of sodium dendrites, but also possessed good electrochemical stability up to 4.7 V and a high ionic conductivity even at low temperature (1.59×10^{-4} S cm^{-1} at ambient temperature and 2.85×10^{-6} S cm^{-1} at −35 °C). Consequently, the assembled Na‖PFSA-Na-SPE‖Na symmetric cell exhibited excellent cycling reversibility of 300 h at 0.5 mA cm^{-2} (room temperature). The SPE was further assembled into a full cell with Na metal anode and Prussian blue (HQ-NaFe) cathode, which delivered a high reversible specific capacity of over 120 mAh g^{-1} at 0.5 C, rate capability of 87.5 mA h g^{-1} at 8 C, and a long cycling life with a capacity retention of ≈85% after 1100 cycles at 1 C. Surprisingly, the full cell exhibited satisfactory electrochemical performance at low temperature with a discharge capacity of almost 92.0 mAh g^{-1} at −15 °C (76% retention compared to capacity at room temperature) and 100% Coulombic efficiency, demonstrating inconspicuous electrochemical polarization. Moreover, the PFSA-Na SPE still maintained excellent mechanical property at −35 °C, thus effectively preventing short circuit caused by Na dendrites, which provided the possibility for developing low-temperature SPEs.

Sångeland et al.[89] developed a copolymer of poly(caprolactone)-poly(trimethylene carbon) (PCL-PTMC) for Na-ion SPE, because the copolymer-based SPE presented a respectable room-temperature ionic conductivity for Li^+-ion migration.[128] The PCL-PTMC had a lower degree of crystallinity than PEO at room temperature and probably generated weaker complexation with cations. When trimethylene carbon units in PTMC were copolymerized with caprolactone, the crystallinity in PCL was destroyed and more amorphous regions were generated, which was profitable for improving the mobility of Na^+. Finally, with a molar ratio of 80:20, the SPE delivered a maximum conductivity above 10^{-5} S cm^{-1} at 25 °C and a cationic transference number of ca. 0.5 at 80 °C. With a hard carbon anode and a Prussian blue cathode, the battery cycled more than 120 cycles at 22 °C, which proves the application prospect of PCL-PTMC in solid-state SIBs.

The conventional solution casting method for preparing SPE membranes may influence the coulombic efficiencies (CE), and the residual liquid solvent in the matrix will lead to irreversible side reactions, too.[63,123,129] Recently, Yao et al.[129] reported an in-situ polymerization process named solvent-free UV-curing, which had the advantages of low operating temperature and fast reaction rate. Before polymerization, the liquid monomer precursor penetrated into the cathode layer, which enhanced the contact between the electrolyte–electrode interface as the curing process went on.[130] They employed poly(ethylene glycol) methyl ether methacrylate (PEGDMA) as a monomer precursor, NaFSI and 2,2-dimethoxy-2-phenylacetophenone (DPMA) as Na salt and photoinitiator respectively.

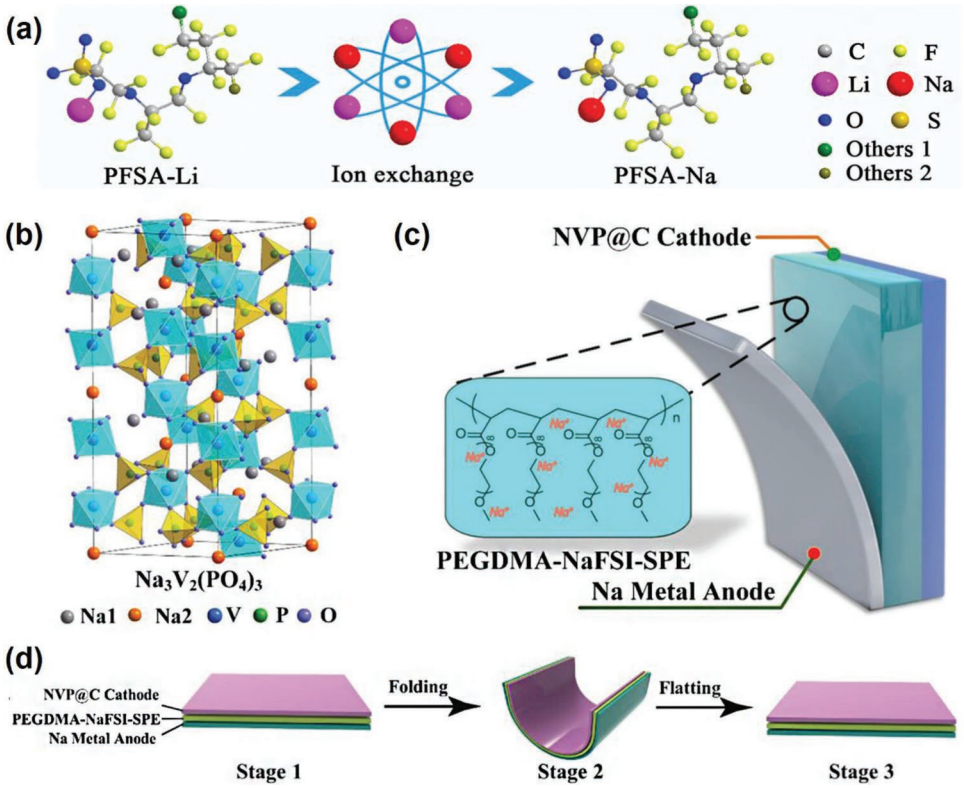

Figure 6. a) Ionic-exchange process of PFSA-Na. Reproduced with permission.[127] Copyright 2019, Wiley-VCH. b) The crystal structure of $Na_3V_2(PO4)_3$. The construction architecture c) and the schematic d) of the $Na_3V_2(PO4)_3$@C|| PEGDMA-NaFSI-SPE||Na bendable battery. Reproduced with permission.[129] Copyright 2020, Wiley-VCH.

With carbon-coated $Na_3V_2(PO_4)_3$ as the cathode (Figure 6b) and Na metal as the anode, the battery showed excellent flexibility (Figure 6c,d), electrochemical properties (105 mAh g^{-1} at 1 C) as well as cycling stability (capacity decay of 5.18% over 740 cycles at 0.5 C).

3.2. Gel PEs (GPEs)

Although SPEs endow with both appropriate mechanical strength and flexibility, their relatively low ionic conductivities still remain to be improved. There is another type of PEs called quasi-solid-state GPEs, which concept was first proposed by Feuillade et al.[131] The GPEs are generally obtained by adding plasticizers or solvents into polymer/salt. After the polymer is plasticized, the liquid electrolyte with alkali-metal-salt is trapped in the polymer matrix.[63,91] Different from the SPEs in which the movement of cations only relies on the segmental motion of polymer chains, GPEs allow the movement of cations in both liquid and gel phases.[63,93] Compared with SPEs, GPEs are more like a compromise option with both solid and liquid-phase properties, enabling GPEs to satisfy the requirements of high ionic conductivity and good flexibility, as well as no risk of leakage and volatilization.[132–134] The GPE-based SIBs can also be divided into different types, individually based on different PE matrices of PEO, PVDF-HFP, PMMA, PAN, PVP, etc. To obtain satisfactory electrochemical performance, various strategies have been applied, such as crosslinking, copolymerization, blending, adding inorganic nanofillers or ionic liquids, and so on.[135–140]

3.2.1. PEO-Based GPEs

For solving the low ionic conductivities of PEO-based SPEs at room temperature, quasi-solid-state GPEs are designed by introducing liquid-phase electrolytes, allowing higher ionic conductivities, even though they must be at a compromise of mechanical strength. Hence, studies on PEO-based GPEs mainly focus on improving mechanical strength.

Crosslinking is a good way to improve the mechanical properties of GPEs, and the resultant cross-linking structure can also effectively inhibit the formation of dendrites. Colo et al.[141] prepared a PEO-based crosslinked GPE by a light-induced free-radical polymerization (UV curing) process. The reactive mixture was obtained by mixing $NaClO_4$, PC, PEO, and photoinitiator, then the viscous gel was transferred into a UV curing set-up equipped with an Hg medium-pressure UV lamp after hot-pressed at 90 °C for 15 min, and the reaction mechanism was schematically shown in **Figure 7**a. The as-prepared crosslinked GPE achieved a high ionic conductivity of 1×10^{-3} S cm^{-1} at 25 °C, approximating that of liquid and exhibited a high working potential (4.7 V vs Na^+/Na). Lehmann et al.[142] prepared a PEO-based crosslinked GPE through a

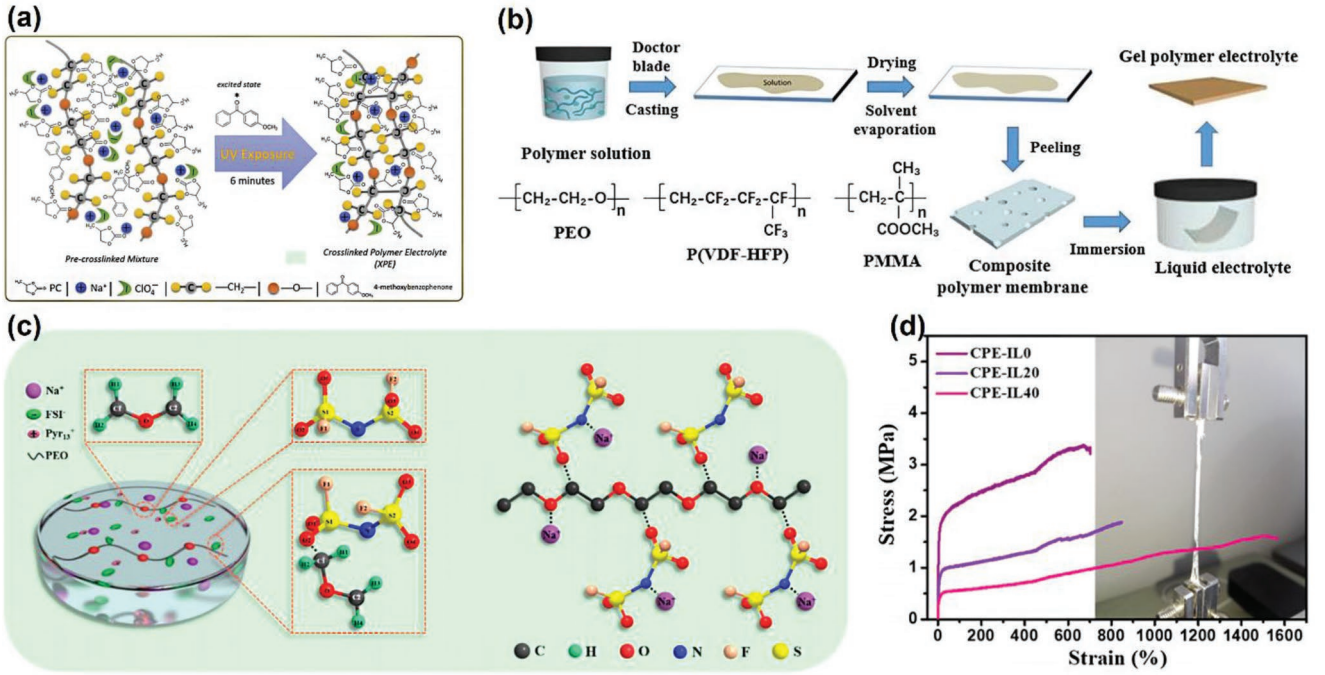

Figure 7. a) Schematic illustration of the reaction mechanism of light-induced crosslinking PE. Reproduced with permission.[141] Copyright 2017, Elsevier. b) The procedure for the preparation of the composite membrane. Reproduced with permission.[132] Copyright 2018, Elsevier. c) Molecular architecture of PEO/$NaClO_4$/$Pyr_{13}FSI$ and d) Stress versus strain curves of PEO/$Pyr_{13}TFSI$ GPE with different $Pyr_{13}TFSI$ content (0, 20, 40 wt% were tagged as CPE-IL0, CPE-IL20, CPE-IL40) and image of stretching test of CPE-IL0. Reproduced with permission. [150] Copyright 2019, American Chemical Society.

single solution-casting technique, showing an ionic conductivity of 2×10^{-4} S cm^{-1} at 20 °C. By adding tetramethylene glycol dimethyl ether (TEGDME), the high crosslinking system kept elasticity under a wide temperature range (constant storage module of ≈1 MPa from 20 to 180 °C). Moreover, the addition of the TEGDME enhanced the ion solvation and led to a lower glass transition temperature (T_g).

Introducing nanofillers in the PEO-based GPEs is also an effective strategy to enhance the performances, such as interfacial characteristics, mechanical stability, and ionic conductivity of SIBs.[143,144] Shi et al.[132] doped SiO_2 into a ternary blending polymer PEO/PMMA/PVDF-HFP to explore the effect of nanofillers on the electrochemical performance of GPEs. The preparation method of the composite membrane was shown in Figure 7b. The results showed that the addition of SiO_2 increased pores in the polymer matrix, enhanced the segmental movement of polymer chains, and expanded the amorphous regions of polymers. The obtained PEO-based composite GPE delivered an ionic conductivity of 0.81×10^{-3} S cm^{-1} at 25 °C. Moreover, it was also suggested that the existence of nanoparticles could stabilize the interface between the GPE and Na-metal anode, improve the mechanical strength of the GPE, and thus contribute to a stable SEI film and a better cycle stability.

Ionic liquids, with the merits of nonflammability, high ionic conductivity, and good electrochemical stability, are suitable plasticizers for preparing GPEs.[137,145–148] Pyrrolidinium-based ionic liquids combining with $TFSI^-$ or FSI^- were widely applied owing to their high antireducibility. It has been demonstrated that the $Pyr_{13}TFSI$ or $Pyr_{13}FSI$ ionic liquids could suppress the crystallization of PEO,[149–152] which had a distinct plasticizing effect on the polymer, but the plasticizing mechanism was seldom discussed. Very recently, Chen et al.[150] prepared a GPE for $Na_3V_2(PO_4)_3$||Na SIB by combining $Pyr_{13}FSI$ with PEO/$NaClO_4$, and the plasticizing mechanism of $Pyr_{13}FSI$ was investigated. It was clarified that the O atoms belonging to the FSI^- anions tended to bind with the particular C atoms on the main chain of PEO, and hence to form a broken branch chain (Figure 7c). As a result, some FSI^- anions attached to the PEO matrix, which provided more Na^+ coordination sites, contributing to a higher Na-salt solubility as well as higher ionic conductivity (6.8×10^{-5} S cm^{-1} at room temperature). They also suggested that increasing the ionic liquid content improved the viscosity and ductility of GPE, but reduced the tensile strength accordingly (Figure 7d); the optimal ratio of $Pyr_{13}FSI$ was 40 wt% for ensuring high ionic conductivity and appropriate mechanical strength. Finally, assembled with $Na_3V_2(PO_4)_3$/Na as cathode/anode and PEO/$NaClO_4$/40 wt% $Pyr_{13}FSI$ as GPE, the battery exhibited a discharge capacity of 108 mAh g^{-1} at 0.1 C and capacity retention of 86.7% after 70 cycles.

3.2.2. PVDF-Based GPEs

Compared with PEO, PVDF has a larger polarity and dielectric constant, which can effectively dissociate Na salts. As a PE matrix, it exhibits excellent properties, including high mechanical strength, electrochemical stability, thermal stability, etc.[147,153–155] Lately, Janakiraman et al.[156] prepared a PVDF-based GPE for SIBs by electrospinning method with a nanofibers structure, which exhibited a wide voltage window (0–5 V vs Na^+/Na) and

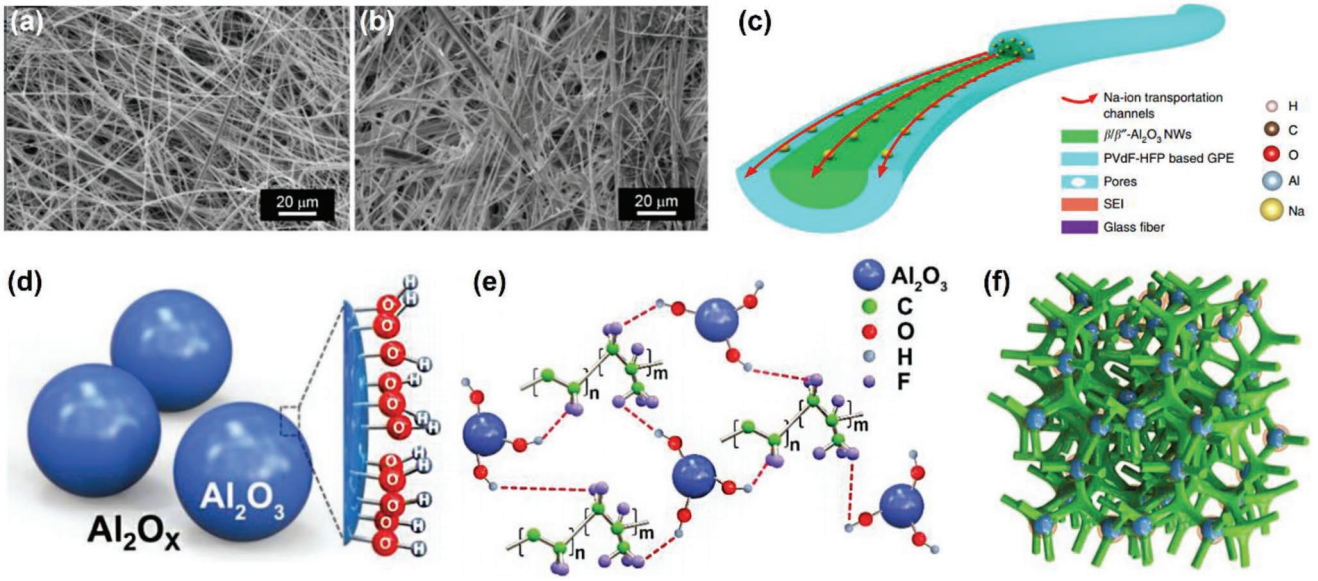

Figure 8. ANs/PVDF-HFP GPE: SEM images of GFs a) without and b) with PVDF-HFP covering. Reproduced with permission.[163] Copyright 2015, Wiley-VCH. c) Structure and Na^+-ion transportation mechanism of ANs/PVDF-HFP GPE. Reproduced with permission.[81] Copyright 2019, Nature. PHP5A GPE: 3D molecular structure diagram of d) Al_2O_3 nanoparticles with hydroxyl on the surface, e) detail diagram and f) skeleton diagram of the quasi-solid-state polymer PHPA formed by Lewis acid–base intermolecular bonding between PVDF-HFP and Al_2O_3 nanoparticles; Reproduced with permission.[164] Copyright 2019, Wiley-VCH.

high ionic conductivity of 1.08×10^{-3} S cm^{-1}. More importantly, PVDF-HFP has attracted considerable attention since Pasquier et al.[157] reported a GPE for LIBs in 2000. By introducing amorphous functional group -HFP into crystalline phase PVDF, PVDF-HFP retained the good mechanical strength of PVDF, while the crystallinities and T_g were reduced significantly. Wang et al.[158] constructed the first quasi-solid-state Na-ion capacitor by using PVDF-HFP as a matrix, which was comparable with those of Li-ion capacitors. With the microporous graphene (MG) and disordered carbon (DC) serving as cathode and anode, respectively, the capacitors showed a high voltage of 4.2 V with an energy density of 168 Wh Kg^{-1}, and it also maintained 85% specific capacitance after 1200 cycles.

Besides, matrix materials such as nonwoven fabrics, glass fibers (GFs) were also exploited to improve mechanical strength.[159–162] Gao et al.[163] used GFs as scaffold covered by PVDF-HFP to prepare a composite GPE, the porous structure of GFs provided micrometer-sized channels as well as enhanced mechanical strength. **Figure 8**a,b shows the SEM images of GFs with and without PVDF-HFP covering. On the other hand, aiming to modify the hydrophobic property of PVDF-HFP, a very thin hydrophilic coating of polydopamine (PDA) was introduced to regulate the surficial performance of the PVDF-HFP polymer. As a result, the as-prepared GPE (1 M $NaClO_4$ in PC/GF/PVDF-HFP/PDA) showed an ionic conductivity of 5.4×10^{-3} S cm^{-1} at 25 °C and a stable voltage up to 4.8 V (vs Na/Na^+). Moreover, GFs played a crucial role in improving thermal stability and mechanical strength (maintain 30 min at 200 °C with stress of 21.6 MPa and strain of 2.9%).

Recently, Lei et al.[81] prepared a novel GPE (ANs/PVDF-HFP) consisting of ion-conductive, cross-linked β/β''-Al_2O_3 nanowires (ANs) covered with PVDF-HFP. The structure and Na-ion transportation mechanism of ANs/Al_2O_3/PVDF-HFP GPE were shown in Figure 8c. The ANs serving as a structural matrix enhanced the density and uniformity of solid–liquid hybrid Na-ion transportation channel for homogenous Na deposition. The as-prepared ANs/PVDF-HFP GPE delivered an ionic conductivity of 7.13×10^{-4} S cm^{-1} at room temperature but lower than GFs/PVDF-HFP that of 9.46×10^{-4} S cm^{-1}, which might be ascribed to the lower liquid electrolyte absorption caused by less porous structure and higher surface area. The assembled battery with $Na_3V_2(PO_4)_3$/Na as cathode/anode and ANs/PVDF-HFP GPE exhibited excellent cycle stability with a capacity retention of 78.8% after 1000 cycles, three times higher than that based on the GFs/PVDF-HFP GPE, which should be attributed to the formation of SEI as well as the homogeneous plating/stripping of Na^+ due to the stable interface between Na-metal anode and the GPE.

Xie et al.[164] reported a 3D structure GPE (PHP5A) comprised of cross-linked 3D structure PVDF-HFP embedded with Al_2O_3 nanoparticles (Molecular structure diagram were shown in Figure 8d–f), which presented both excellent flexibility and wide working temperature range (-20 to 70 °C). The porous 3D structure facilitated the fast ionic migration (ionic conductivity up to $\approx 1.3 \times 10^{-3}$ S cm^{-1}) and enabled uniform distribution of electrochemical stress on the Sn anode during the process of charging/discharging. The existence of uniformly distributed Al_2O_3 nanoparticles expanded the amorphous region of the polymer matrix and enhanced the mechanical strength of GPE.[165] With graphite and Sn foil as cathode and anode respectively, the DIB exhibited a high capacity of 96.8 mAh g^{-1}, good rate capability, and excellent cycling stability with a capacity retention of 97.5% after 600 cycles at a high current rate of 5 C.

3.2.3. GPEs Based on Other Polymer Matrices

Some polymers, such as PMMA, PAN, and PVP, have been also reported to serve as polymer matrices for GPEs.[166–172] These polymers also present different disadvantages. For example, PVP-based GPEs generally deliver lower ionic conductivities because PVP also is a semicrystalline polymer despite its good film-forming ability. PAN-based GPEs endow with low mechanical strength and weak film-forming ability. PMMA-based GPEs are believed to present inferior interface stability as well as cycle performance.[24,82] Nevertheless, due to the individual advantages (such as good affinity with organic electronics, amorphous nature of PAN; wettability, higher mobility and concentration of charge carriers of PMMA; optical properties and mechanical strength of PVP),[165,173–175] the polymers are supposed to attain better application in Na^+-ion GPEs by different strengthening methods. Therefore, some modification strategies have been proposed to improve their comprehensive performance.

Recently, based on the composite design of PMMA and PVDF-HFP, Mishra et al.[165] prepared a PMMA/PVDF-HFP/EC/PC/$NaCF_3SO_3$ system with nano-Al_2O_3 as additive. PVDF-HFP with good liquid-retention capability could match with amorphous phase PMMA, and the blended GPE showed superior ionic conductivity. As the content of nano-Al_2O_3 increased to 6 wt%, an ionic conductivity of 1.5×10^{-3} S cm^{-1} was obtained at room temperature. In addition to this, Chandni et al.[176] tried to combine PEO with PAN, which exhibited an ionic conductivity of about $\approx 10^{-4}$ S cm^{-1} (EO/AN: Na = 20, 20 wt% TiO_2).

Kumar et al.[174] added SiO_2 nanofillers into PMMA/$NaClO_4$/EC/PC system. With controlling SiO_2 content range from 0 to 25 wt%, the maximal ionic conductivity of GPE was 3.4×10^{-3} S cm^{-1} when the SiO_2 content was optimized at 4 wt% (20 °C). The GPE presented a wide electrochemical window of about 5 V and stayed stable over the temperature range of –80 to 140 °C, which proved the potential of PMMA for application in SIBs. Similarly, Rao et al.[175] used ZrO_2 as nanofillers to construct PVP/$NaPO_3$/ZrO_2 GPE, which also delivered a high ionic conductivity of 2.14×10^{-3} S cm^{-1} for Na^+-ion transfer at room temperature.

The existence of C=N groups in polymer materials is beneficial to boost the transfer of active cations.[177] Hence, PAN with C=N groups was exploited to replace C=O active groups in PEO. Osman et al.[170] prepared a system of PAN/24 wt% $NaCF_3SO_3$, which had an ionic conductivity of 7.13×10^{-4} S cm^{-1} at room temperature, even higher than that of 3.04×10^{-4} S cm^{-1} of Li-ion system (PAN/26 wt% $LiCF_3SO_3$), which was attributed to the weaker interaction between Na^+ cations and the unique N atoms in PAN, promoting the migration of Na^+ ions. Lately, Manuel et al.[97] reported a PAN-based GPE, in which 1 M $NaClO_4$ dissolved in an organic solvent (EC/PC/DME = 1/1/1 in volume ratio), and PAN serving as the PE matrix, which presented an ionic conductivity of 3.01×10^{-3} S cm^{-1} at room temperature. Assembled with a nanocomposite (polyimide (PI)/multiwalled carbon nanotube (MWCNT)) as the cathode and Na metal as the anode, the obtained battery with PAN-based GPE delivered an initial discharge capacity of 98 mAh g^{-1}, which slightly increased to 100 mAh g^{-1} after a few stabilization cycles and 82.5 mAh g^{-1} was remained after 3000 cycles (about 84% of the initial discharge capacity).

Recently, Xu et al.[44] reported a multifunctional GPE based ethoxylated pentaerythritol tetraacrylate (EPTA) by in situ thermal polymerization method. The EPTA could regulate anion and cation fluxes to homogenize the Na plating and make anion intercalation smoothly. They adopted PC: EMC (1:1, v:v) plasticizer with FEC as cosolvent and 1,3-pro-panesultone (PS) as an additive, which facilitated the formation of SEI/cathode electrolyte interphase (CEI) on the anode/cathode side, bringing about stable cycle performance and a wider electrochemical window. The $NaPF_6$/EPTA/PC/EMC/FEC/PS system exhibited high ionic conductivity of 5.33×10^{-3} S cm^{-1} at 25 °C and wide electrochemical stable voltage window up to 5.5 V versus Na/Na^+. With graphite and Na metal as cathode and anode, respectively, the sodium-based DIB delivered a high energy density of 484 Wh Kg^{-1} with an operation voltage of 4.4 V and capacity retention of 86.7% (78 mAh g^{-1}) after 1000 cycles.

4. PEs for K-Ion batteries

In the previous section, we reviewed the progress of PEs for SIBs and summarized the classification of different types of polymers. The PEs employed in SIBs effectively solve some problems existing in liquid-phase electrolytes and solid-phase ISEs. In contrast, fewer studies have been made on KIBs based on PEs. Compared with the Na^+ ion radius (0.97 Å), K^+ ion has a larger ion radius (1.33 Å), which limits the choice of electrodes. However, the electrochemical redox potential of K^+/K is more close to Li^+ (–2.93 V of K^+/K and -3.04 V of Li^+/Li), so that KIBs can theoretically deliver a higher working platform.[56,178] Moreover, potassium has good flexibility, enabling better contact between materials and can expand the application field of technology.[68,179,180] Therefore, KIBs also have good research value and application potentials. Growing attention has been being paid to K^+-conductive PEs (KCPEs) for KIBs (inset in Figure 1b,d). However, so far, there are just a few studies on KIBs based on PEs. In this section, we summarized the progress of PEs for KIBs by classifying the existing KCPEs into single polymer-based PEs and performance improvement methods.

4.1. Recent Progress on Single Polymer-Based Electrolytes

4.1.1. PEO-Based PEs

PEO-based electrolytes have been developed into various research fields of metal-ion batteries, including KIBs (**Table 4**). The potassium salt is an important component of electrolytes, and the proper addition of potassium salt can improve the amorphous fraction of polymer. The structure and properties of the polymer can also be changed by dissolving the appropriate salt.[181] Chandra et al. prepared a SPE film [(1-*x*)PEO: *x*KBr ($0 < x < 50$ wt%)] by using a fast and solvent-free/dry-hot-pressing technique. As observed in **Figure 9**a, the conductivity of the SPE film increased as the concentration of KBr increased gradually. Because the crystallinity of the polymer decreased along with the increasing complexation of salt and electrolyte, and the segmental chain movement became easier. Then,

Table 4. Performance parameters of single polymer-based electrolytes for KIBs.

Electrolyte composition	Ionic conductivity [S cm^{-1}]	Electrochemical stable voltage [V]
PEO/$KBrO_3$[28]	7.74×10^{-8}	–
PEO/KBr[183]	5.0×10^{-7}	–
PEO/CH_3COOK[185]	2.74×10^{-7}	–
PEO/KFSI[68]	2.7×10^{-4} at 60 °C	–
PVP/KIO_3[186]	1×10^{-9}	–
PVA/KCl[184]	9.68×10^{-7}	–
PVA/KBr[181]	1.23×10^{-5}	–
PUA/KI[187]	1.59×10^{-4}	2 V
PPCB/KFSI[24]	1.36×10^{-5}	4 V
P(AHG)/KI[182]	3.41×10^{-4}	–

the maximum conductivity (5.0×10^{-7} S cm^{-1}) was obtained when the weight ratio of PEO/KBr was 70:30. As the concentration continued to increase, the conductivity decreased, possibly ascribable to ion binding.[182] Besides, when the mass ratio of KBr was greater than 50%, the prepared electrolyte membrane was fragile.[183,184] Similarly, Agrawal et al. studied the effect of potassium acetate (CH_3COOK) concentration on the conductivity of PEO-based polymers.[185] A poly(ethylene oxide)-potassium acetate (PEO-CH_3COOK) SPE was prepared via a hot-press cast method and delivered an ionic conductivity of 2.74×10^{-7} S cm^{-1} at room temperature when the PEO/CH_3COOK weight ratio was 95:5.

This phenomenon shows that different salts may have different effects on the same polymer body. It has been found in common organic solvents that the metal salts with larger anions have lower lattice energy and stronger solubility, which is conducive to improving the ionic conductivity.[82] Based on this, Feng et al. prepared (PEO_m-KFSI) GPEs with different mole ratios ($m = n_{[PEO]}/n_{[KFSI]}$) using KFSI salt with large anionic groups. At 40 °C, the ionic conductivity reached its peak (1.14×10^{-5} S cm^{-1}) when the molar ratio of (EO)/K^+ was 10, as shown in Figure 9b. Further, the SPE was assembled into a full cell with the configuration of K‖PEO-50%KFSI‖Ni_3S_2@Ni. In the voltage range of 0.01–3 V at 40 °C, the full cell delivered a high initial reversible capacity (312 mAh g^{-1} at 25 mA g^{-1}), stable cycling performance (capacity retention of 98% after 100 cycles) at 25 mAh g^{-1}. In a comparative experiment using conventional organic electrolyte 1 M KFSI in EC/DEC (v/v, 1:1), after 20 cycles, the capacity drops to 24 mAh g^{-1} (Figure 9c). It was demonstrated that the application of PEs not only improved the safety facing organic liquid electrolyte, but also limited the diffusion of sulfide in the organic electrolyte, and improved the cycling performance of KIBs.[68]

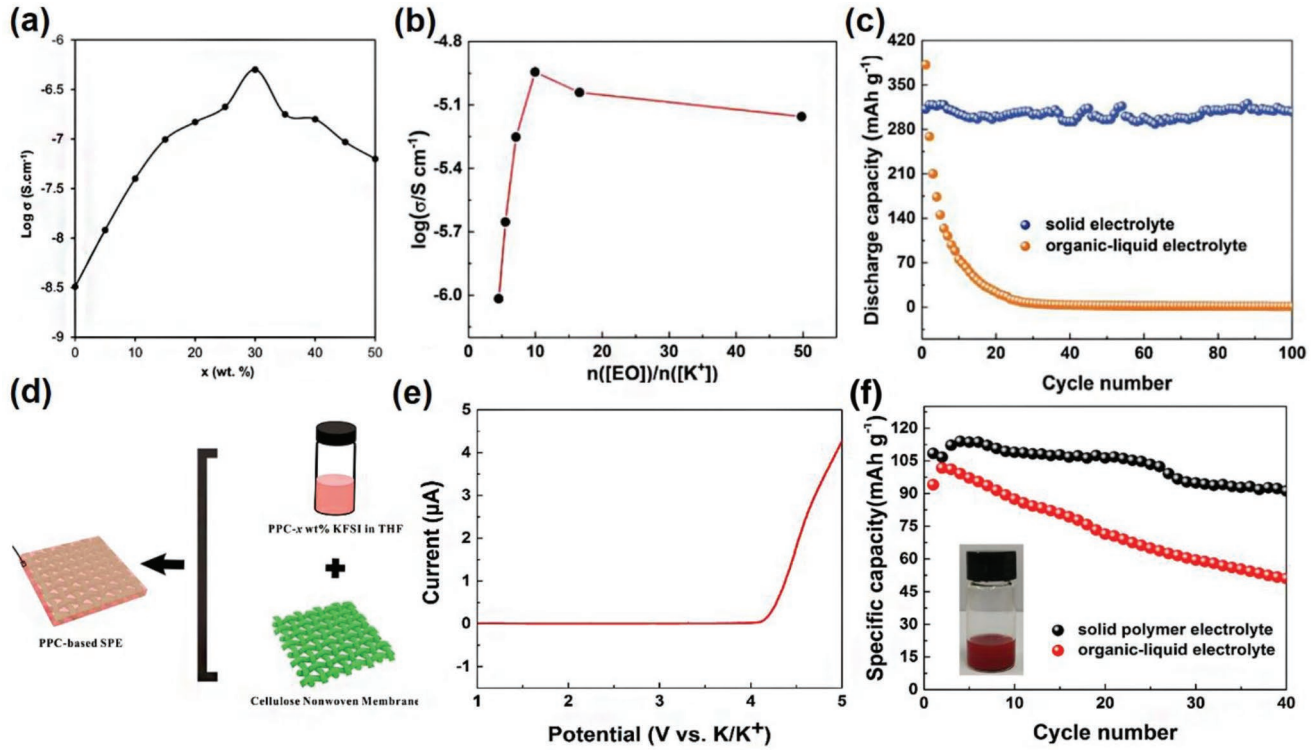

Figure 9. a) "Log *r*–*x*" plot for the hot-pressed SPEs: (1-*x*) PEO:*x*KBr, where *x* is weight percent. Reproduced with permission.[183] Copyright 2015, Springer Nature. b) Ionic conductivity of the PEO/KFSI SPE with the varied molar ratio of [EO]/[K^+] at 40 °C. c) Comparison of cycling performance using 3 h Ni_3S_2@Ni electrode between PEO-based SPE and the organic-liquid electrolyte at a current density of 25 mAh g^{-1}. Reproduced with permission.[68] Copyright 2019, Elsevier. d) Synthesis of PPCB-KFSI SPE. e) LSV results for the SPE. f) Cycling performance of PTCDA with PPCB-KFSI SPE or organic-liquid electrolyte at a current density of 20 mA g^{-1}. The inserted digital image is the solubility test of PTCDA in 1 M KFSI in EC/DEC (v/v, 1:1) electrolyte. Reproduced with permission.[191] Copyright 2018, Elsevier.

4.1.2. Polyester-Based PEs

Polycarbonate polymers with strong polar groups ([−O−(C=O) −O−]) have attracted wide attention (Table 2).[188] For example, Cui et al. developed a SPE supported by fiber nonwoven fabric and used poly(propylene carbonate) (PPC) as ion transport materials in LIBs, which positively affected performance study of full battery $LiFePO_4$||Li.[189] Inspired by this, Feng et al.'s team applied this method to prepare a PPCB-KFSI SPE with a 3D continuous and uniform structure, as shown in Figure 9d. The Na^+-based SPE delivered a maximum conductivity (1.36×10^{-5} S cm^{-1}) when the salt concentration reached 18 wt% at 20 °C. Besides, they studied the plating/stripping behavior of K^+ ions in the electrolyte with cyclic voltammetry. The strong reduction peaks appeared at -0.3 V (vs K/K^+) and the strong oxidation peak appeared at 0.21 V (vs K/K^+). It was shown that the SPE had an electrochemical window of 4.15 V, which demonstrated excellent electrochemical stability in Figure 9e. Moreover, assembled with organic perylene-3,4,9,10-tetracarboxylic dianhydride (PTCDA) cathode, a full cell (K||PPCB-KFSI SPE||PTCDA) showed an excellent rate performance. Under the voltage range of 1.5–3.5 V (vs K/K^+), the battery could remain 84.3% of the initial capacity after 40 cycles at 20 mA g^{-1}, superior to the conventional organic electrolyte (Figure 9f). Because the SPE could effectively inhibit the dissolution of active organic substances, irreversible side reactions, and other interfacial problems.[24]

Polyurethane (PU) (−[NH−(C=O) −O]$_n$−), synthesized by polymerizing polyol and diisocyanate, has a unique two-term structure consisting of soft segments and hard segments. The former originated from polyols, contributing to dissolve cations, and the latter comprises diisocyanate, boosting the electrochemical stability.[190] Considering that the characteristic of N−H, C=O, and C−O−C groups in PU body can coordinate with K^+, Rayung et al. used nonedible jatropha vegetable oil, 2,4-tolylene diisocyanate (TDI), and 2-hydroxyethyl methacrylate (HEMA) to synthesize a polyurethane acrylate (PUA)-based PE, which presented an optimal ionic conductivity of 1.59×10^{-4} S cm^{-1} at room temperature. But the electrochemical window of this electrolyte was only 2 V according to the consequence of LSV, which limited the choice of the cathode and the energy density of the full battery.[187]

4.1.3. Others

PVP is also a typical polymer matrix for PEs. Rao et al. prepared a PE of PVP/KIO_3.[186] At room temperature, the maximum ionic conductivity was only 1×10^{-9} S cm^{-1} when the weight ratio of PVP/KIO_3 was 70:30. Although the PVP-based PE could promote the dissociation of metal salts but had poor ionic conductivity, which could be solved by blending and other methods. The hydroxyl group on the PVA carbon chain skeleton can be used as a source of hydrogen bonds. Ravi et al. prepared PVA/KCl and PVA/KBr PE films by solution casting. It was found that at room temperature, the best ionic conductivity at 15 wt% salt concentration was 9.68×10^{-7} and 1.23×10^{-5} S cm^{-1}, respectively. The ionic conductivity of the two saline electrolytes differed by nearly an order of magnitude.[181,184]

Due to the advantages of natural source, good biodegradability, low toxicity, and low cost, polysaccharide polymers have also been exploited for PEs in KIBs. Sago starch is a polysaccharide polymer formed by the polymerization of anhydrous glucose (AHG).[182] Rhee et al. prepared a biopolymer electrolyte using sago starch and potassium iodide (KI) with a weight ratio of 50:50, which delivered an optimal ionic conductivity of 1.59×10^{-4} S cm^{-1} at room temperature. Although this environmentally friendly biopolymer electrolyte with high ionic conductivity was successfully synthesized, the practical application in KIBs remained to be further studied. Based on the good progress in SIBs with polysaccharide polymers, it's believed that it can be further developed in KIBs.[182]

Although some single polymer-based electrolytes have good performance, the performance of most single polymer-based electrolytes (mainly ionic conductivity) is still difficult to meet the requirements of applications. For example, pure PEO-based PEs have only 10^{-7} ionic conductivity. Therefore, some methods have been adopted by researchers to improve the performance of the electrolytes.

4.2. Methods to Improve the Performance of PEs

In order to meet the performance requirements of PEs for KIBs, the researchers have devoted many efforts to improve the ionic conductivity through polymer blending,[192–195] copolymerization,[196] introducing inorganic fillers,[197–199] and the addition of plasticizer,[200] which focused to reduce the crystallinity of the polymer matrices and to increase the chain movement (**Table 5**).

4.2.1. Blending and Copolymerization

The advantages of the blending polymer matrices include facile preparation process and controllable physical properties by mixing two or more polymers and adjusting their proportion.[194] Blending is one of the effective methods to improve amorphous properties.[195] Some studies on the blending polymer matrices in KCPEs systems have also been implemented.

Table 5. Performance parameters of improved PEs for KIBs.

Electrolyte composition	Ionic conductivity [S cm^{-1}]	Electrochemical stable voltage
PEO/PVA/KIO_3[193]	4.77×10^{-6}	–
PEO/PVC/KBr[195]	2.56×10^{-5}	–
PEO/PVC/KCl[194]	8.29×10^{-6}	–
PVP/PVA/KIO_3[192]	1.22×10^{-5}	–
PECH-g-POEM/KI[196]	3.7×10^{-5}	–
PEO/KI/CeO_2[199]	2.15×10^{-3}	–
PEO/KBr/SiO_2[198]	2.5×10^{-5}	–
PEO/KNO_3/KI[197]	6.15×10^{-6}	–
PMMA/KPF_6/EC:DEC:FEC[179]	4.3×10^{-3}	4.9 V
PAN/KI/EC[200]	2.089×10^{-5}	–

The most commonly used PEO-based PEs generally have low ionic conductivity at room temperature. Reddeppa et al. mixed PEO with PVC and complexed with KBr and KCl, respectively, to prepare a KCPE and conduct performance research.[194,195] In the PEO/PVC blend system doped with KBr, the ionic conductivity gradually increased with the increase of KBr concentration and temperature, and showed ionic conductivities of up to 2.56×10^{-5} S cm^{-1} under room temperature at the PEO/PVC/KBr weight ratio of 42.5:42.5:15. The results of PEO/PVC/KCl electrolyte blends were similar. The maximum ionic conductivity (8.29×10^{-6} S cm^{-1}) was found at the mass ratio of 42.5:42.5:15. Compared with the pure PEO-based KCPE, the ionic conductivity was improved. The -OH group of PVA was even more conducive to the blending of the polymer, Bhargav et al. developed a PEO/PVA blend system by doping with KIO_3.[193] The T_g of PEO/PVA polymer decreased with the increase of KIO_3 concentration (66 °C for pure PEO/PVA electrolyte and 54.5 °C for PEO/PVA/30% KIO_3 electrolyte). At room temperature, the maximum ionic conductivity was 4.77×10^{-6} S cm^{-1}, and the mass ratio is 42.5:42.5:15. Sharma et al. developed the blend PE (PVP/PVA/KIO_3 35:35:30, w/w/w) with ionic conductivity of 1.22×10^{-5} S cm^{-1} at room temperature. Compared with the work (PVP/30% KIO_3) with ionic conductivity of only 1×10^{-9} S cm^{-1}, the ionic conductivity was greatly improved.[192] It follows that the blending design strategy can effectively improve the ionic conductivities of KCPEs.

Compared with blending polymer matrices, the method of synthesizing copolymers is more complicated.[195] The copolymers are composed of two or multiple chains with different chemical properties. The net repulsion between the chain segments leads to the local separation structure at the nanometer level, which can well control the ion transport and the mechanical properties of the film.[196] When metal salts are added to these copolymer matrices to form a rubber-like solid, they still have high ionic conductivities. Via an atom transfer radical polymerization (ATRP) method, Kim et al. synthesized a comb polymer (PECH-*g*-POEM). The polymer consisted of the main PECH chain and the side chain POEM (mass ratio: 60:40). The chlorine atom in the main chain was used as the starting site and grafted with the side chain. KI was added to the polymer matrix, and the ionic conductivity (3.7×10^{-5} S cm^{-1}) at room temperature reached the highest value when the concentration reached 15 wt%.[196] The good electrochemical properties of the KCPEs indicate that the copolymerization method is promising.

4.2.2. Inorganic Fillers

The preparation of commixture KCPEs by adding inorganic fillers can also improve the ionic conductivity. There have been many reports on other metal ionic electrolytes. Inorganic fillers can be divided into two types according to their contributions: passive and active fillers. Passive fillers (Al_2O_3, SiO_2, TiO_2, etc.) can not only improve the mechanical properties of PE, but also improve the ionic conductivity of PE because of their Lewis acid surface groups and large specific surface areas. Active fillers are involved in the transport of K^+ and contribute to conductivity, and induce complex conductive behavior.[88,201]

De et al. studied the effect of CeO_2 nanoparticle (size ≈ 10 nm) on the morphology and ionic conductivity of PEO/KI KCPE.[199] As shown in **Figure 10**a, pure PEO presented a regular crystal network. After the addition of KI, salt complexation with PEO destroyed the crystal structure. With the addition of CeO_2, the morphology of the PEs became flatter (Figure 10b). The good microstructure could improve ion conductivity. The ratio of PEO/KI was kept at 80:20 and 85:15, and the influence of different proportion of CeO_2 on the conductivity was studied (Figure 10c). Figure 10c shows the presence of two conductivity maxima. When the content of CeO_2 was less than 5 wt%, the osmotic conduction paths were formed around the nanoparticles, and the *trans*-arrangement of PEO improved the ionic conductivity of the KCPE. When the content of CeO_2 was between 5 and 10 wt%, the interaction between Lewis acid and base led to gauche arrangement of PEO main chains, which inhibited the PEO phase motion and reduced the ionic conductivity; Above 10 wt%, CeO_2 interacted with the ether oxide groups (solvated with K^+), weakened their binding with K^+, and improved the conductivity. When 20 wt% CeO_2 was added, the ionic conductivity reached the highest value (2.15×10^{-3} S cm^{-1}). Compared with the pure-PEO/KI system (1.53×10^{-5} S cm^{-1}) at room temperature, the ionic conductivity increased by two orders of magnitude. When CeO_2 concentration was too high, its strong interaction with PEO could lead to the increase of polymer matrix crystallinity.

Besides, the nanoparticle SiO_2 (size ≈ 8 nm) was also used to prepare the K^+ conducting composite KCPE. Chandra designed a composite SPE by mixing ((1–*x*) [70PEO:30KBr] with nanoparticle SiO_2.[198] The influence of the composition and temperature on the conductivity of the KCPE was investigated (Figure 10d). The results showed that the ionic conductivity of [95 wt% (70PEO:30KBr) +5 wt%SiO_2)] KCPE was 2.5×10^{-5} S cm^{-1}. Compared with their previous work (70PEO:30KBr), the KCPE delivered an increased conductivity by two orders of magnitude, which was ascribed as that the interaction between the PEO backbone and the SiO_2 filler provided more jump sites for K^+ and promoted ion migration.

Agrawal et al. found in their study on PEO/KNO_3 KCPEs that when the mass ratio was 95:5 and 70:30, the KCPE had a high ionic conductivity at room temperature of 2.76×10^{-7} S cm^{-1} and 4.31×10^{-7} S cm^{-1}.[197] Based on these two KCPEs, they used KI as an active filler and adopted two different strategies to improve ionic conductivity. For the first approach involved physical/hot mixed process, in which the different mass fractions of KI (as second–phase filler dispersoid) were dispersed into the PEO matrix, and this could increase the fraction of amorphous PEO. Using this method, the conductivity of both CPEs ions was improved. The ionic conductivity at room temperature of [(95 wt%PEO + 5KNO_3) + 7 KI] and [(70PEO + 30KNO_3) + 10 KI] KCPEs was 6.15×10^{-7} and 3.98×10^{-7} S cm^{-1}. The ionic conductivity increased by an order of magnitude. The second method was to mix KNO_3 and KI according to the optimal ratio obtained by the previous method, and then to grind the balls at different times followed by a hot pressing method to prepare CPEs. The results showed that the nano-ionic effect at the boundary of KNO_3 and KI phase could be induced by ball grinding and the ionic conductivity could be improved.

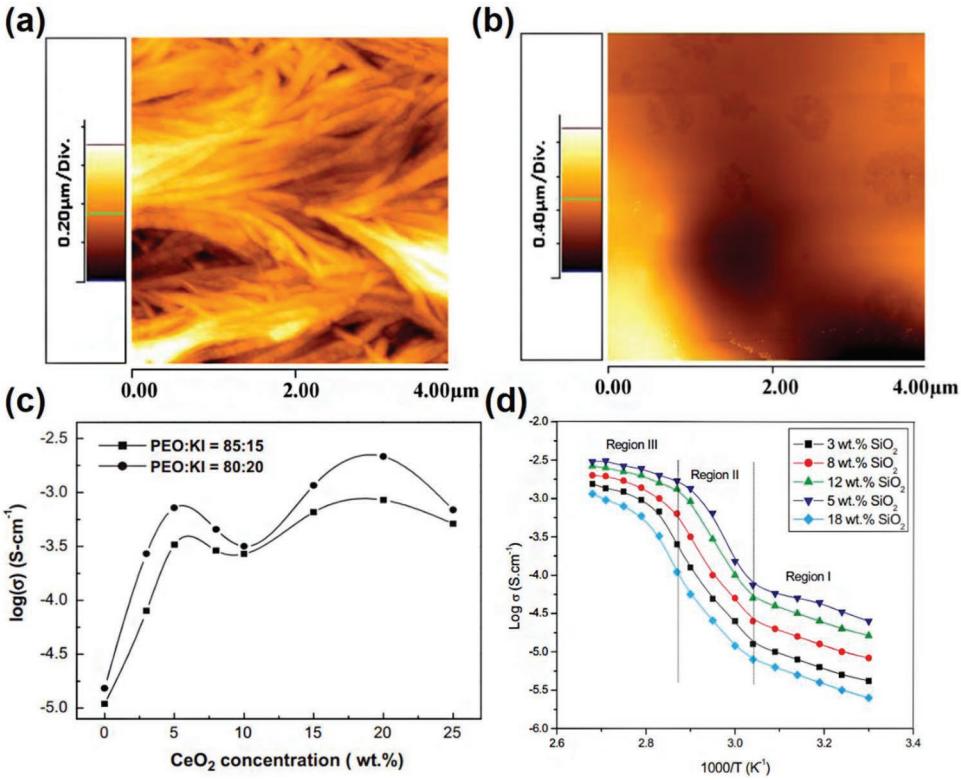

Figure 10. 2D AFM topographic images of a) pure PEO and b) PEO–KI-CeO_2 (20 wt%) composite PE. c) Variation of conductivity with CeO_2 concentrations in the composite PE complex at room temperature. Reproduced with permission.[199] Copyright 2011, Elsevier. d) Temperature-dependent ionic conductivity for NCPE: (1–*x*)(70PEO: 30KBr) + *x*SiO_2, where *x* is wt%. Reproduced with permission.[198] Copyright 2017, Elsevier.

4.2.3. K^+-Based GPEs

K^+-based GPEs synthesized by adding plasticizer are also very promising for KIBs. Goodenough et al. polymerized the monomer methyl methacrylate (MMA) (20.0 mmol) and the cross-linker tetraethylene glycol dimethacrylate (TEGDMA) (1.0 mmol) into crosslinked PMMA using azobisisobutyronitrile (0.03 mmol) as the initiator in the organic liquid electrolyte (0.8 M KPF_6 in EC:DEC:FEC(45:45:10,v/v/v)). It was shown that the PMMA-based GPE had a high ionic conductivity (4.3×10^{-3} S cm^{-1}) and a high voltage window (4.9 V vs K/K^+) at room temperature (**Figure 11**a). The batteries configured with polyaniline/K were assembled with the GPE and traditional organic liquid electrolyte, respectively. Compared with liquid-phase electrolytes, the GPE offered better cycle performance (98% discharge capacity retention rate after 100 cycles at 50 mA g^{-1} and an average coulombic efficiency of 99.3% over the whole cycle) and superior rate capability (Figure 11b,c). Compared with other KIBs, the electrochemical performance of this work was also outstanding. The excellent cycling performance and high coulombic efficiency were mainly attributed to the fact that the KCPE could inhibit the side reactions on the electrode surface and the growth of potassium dendrites, thus establishing a stable interface.[179]

On the basis of the success of a blending GPE membrane in a Li^+-based DIB system,[202] the same group applied a similar approach to prepare a K^+-based GPE membrane (PVDF-HFP/PEO(95:5,w/w) + 1 M KPF_6/EC/DMC/EMC (4:3:2,v:v:v)) and assembled a Sn||AC flexible potassium ion mixing capacitor (PIHC).[203] PVDF-HFP had the advantages of relatively low crystallinity, high ionic conductivity and good mechanical strength. The addition of PEO could form an H-F hydrogen bond with PVDF-HFP, which was beneficial to improve the pore structure. Compared to organic electrolytes (capacity gradually decreased after 400 cycles), PIHC based on the GPE (2000 cycles of stable cycles) showed good cycling stability. SEM characterizations of tin anode suggested that the surface of the tin foil after 500 cycles in the organic electrolyte presented serious pulverization and cracks, while that in the PIHC with the GPE was still relatively smooth and flat after 2000 cycles. Figure 11e shows the advantages of GPEs including a uniform de-/alloying process and mitigation of volume change.

The addition of suitable plasticizers is also significant to improve the ionic conductivity of K^+-based GPE. Kumar et al. prepared a GPE membrane with PAN as a PE matrix and EC as the plasticizer.[200] At 30 °C, the maximum conductivity of PAN/EC/KI (70:30) wt% was 2.089×10^{-5} S cm^{-1}. In the study on the thermal stability of CPEs, it was found that the addition of plasticizer reduced the T_g and T_m values of the GPE, which was conducive to improving the ionic conductivity.

5. Conclusion and Perspectives

For a battery system, the electrolyte is an indispensable part. Polymer electrolytes (PEs) enable the electrolyte to combine the

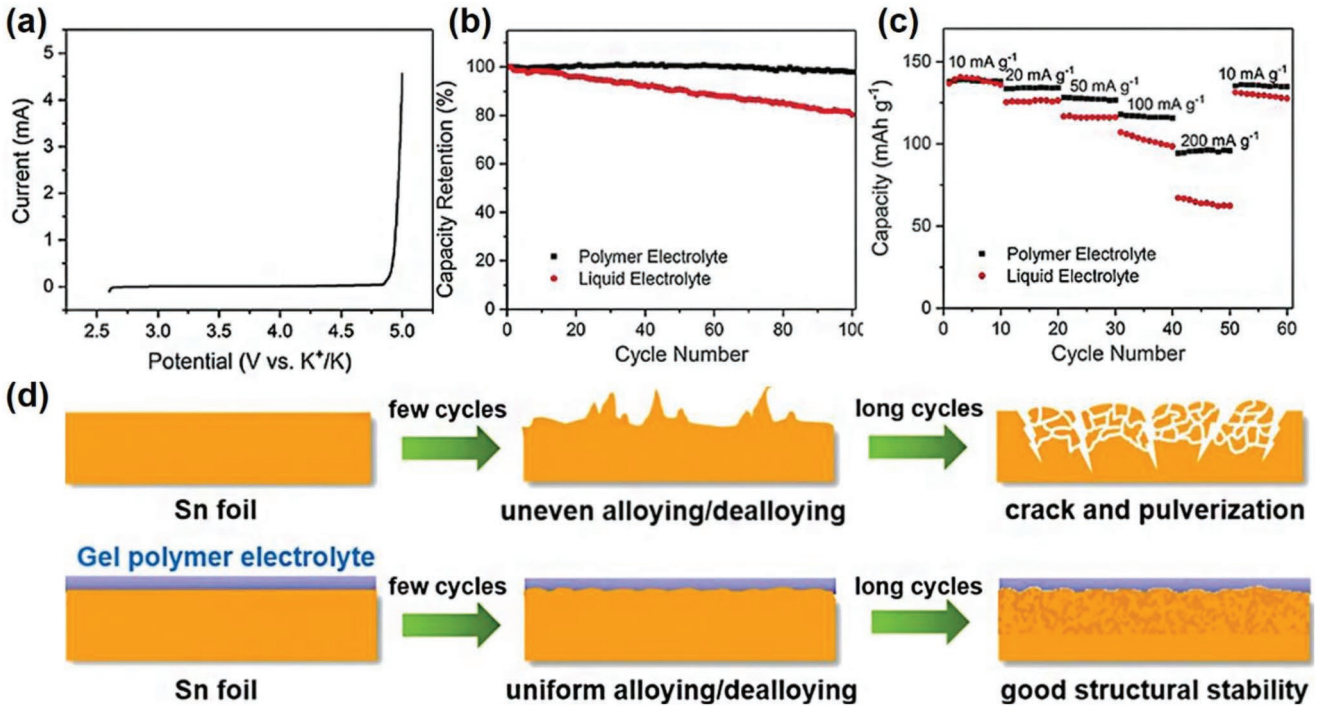

Figure 11. a) LSV plot of the polymer-gel electrolyte against a potassium-metal anode at 1.0 mV s^{-1}. b) Cycling performance of the polyaniline cathode at 50 mA g^{-1}. c) Rate performance of the polyaniline cathode at different current densities from 10 to 200 mA g^{-1}. Reproduced with permission.[179] Copyright 2018, Wiley-VCH. d) Schematic illustration of the failure mechanism of the Sn anode in the liquid electrolyte and the protection mechanism of the gel PE. Reproduced with permission.[203] Copyright 2020, American Chemical Society.

advantages of both rigidity/toughness of solid electrolytes and ionic conductivity of liquid electrolytes. Besides, PEs endow with some other merits of flame-retardancy, no leakage and volatility, thermal/electrochemical stability and flexibility, and show great potential for the application in batteries. Due to the shortage of lithium resources and severe concern of safety, the development of PE-based SIBs and KIBs is a popular trend. At present, the relative researches are still in its infancy, but it is realistic that this field will advance the application of next-generation clean energy in the near future. Therefore, PEs, as a potential electrolyte in SIBs and KIBs, still need further studies. Herein, we enumerated the latest development of PEs and also discussed their working mechanism and modification strategies.

In the past decade, different design strategies, including blending, crosslinking, copolymerization, nanofillers, etc., have been proposed to boost the development toward high-performance Na^+/K^+-based PEs. For PEs, the basic requirements include high enough ionic conductivity (>10^{-4} S cm^{-1}), transference number close to unity, mechanical strength, toughness, wide electrochemical window and stability, good interfacial compatibility with electrodes, etc. Currently, it is noteworthy that the main shortages of Na^+/K^+-based SPEs and GPEs are low ionic conductivity, insufficient mechanical properties, etc., which hinder the ongoing steps toward practical application. It is necessary to modify the electrolyte systems further or develop new PE systems. For example, the next-goal for GPEs might be to enhance their mechanical strength and to increase the porosity of GPEs for containing and maintaining more liquid electrolyte. Furthermore, for SPEs, the low ionic conductivities are the main hurdle remaining to be overcome.

From the perspective of practical application, Na^+/K^+-based PEs should meet some ideal performance requirements for SIBs/KIBs, such as: high ionic conductivity, high cation migration number, appropriate mechanical strength, excellent chemical and thermal stability, etc.

1. High ionic conductivity: Ionic conductivity is an important index to evaluate the performance of PEs and reflects the ability of PEs to transport alkali metal ions (Na^+, K^+). However, as mentioned above, the conductivity of Na^+/K^+-based PEs (10^{-6} to 10^{-3} S cm^{-1}), particularly SPEs, is much lower than that of conventional liquid electrolytes (10^{-3} to 10^{-2} S cm^{-1}), especially at room temperature. The ionic conductivity of the Na^+/K^+-based PEs must be at least 10^{-3} S cm^{-1} in order for SIBs/KIBs to have good cycle and rate performance.[63,82,91] The relevant design strategies include blending, cross-linking and inorganic fillers, plasticizer/solvent addition, etc. Besides, the concentration of salts also has a great influence on PEs, in which too low is unconducive to the generation of energy carriers and too high will affect the structure of molecular skeleton chains.
2. High cation migration number ($T_+ \approx 1$). The cation migration number is a measure of the cation mobility in the PEs relative to the anion.[91] Reverse movement of anions without being deposited on the electrodes can cause concentration polarization, which results in increased internal impedances and reduced discharge voltages. Single ion conductive PE is used to limit the anion and increase the cation conductivity by covalently binding the anion to the polymer chain or adding an anion acceptor.[204] Therefore, how to restrict the migration

of anions in PEs is a key issue. However, note that different from in "rocking-chair" battery systems, in a DIB system, active ions include both cations and anions, which needs a comparable ion transfer kinetics for cations and anions.

3. Appropriate mechanical strength: Good mechanical properties enable the suppression of the dendrite growth, and at the same time, it cannot be as fragile as some inorganic solid electrolytes, which have seldom relaxation elasticity under pressure.[205] PEs based on linear polymer chains have less mechanical properties, especially GPEs (plasticizers are added to improve ionic conductivity). Some methods to improve the mechanical strength of PEs cover crosslinking, inorganic fillers, etc.[201,205]
4. Wide electrochemical voltage window (0–5 V): The oxidation potential should be higher than the intercalation potential of alkali metal ions or anions into the cathode, and the reduction potential should be lower than that of alkali metal ions in the anode. Matching a high voltage cathode material is beneficial to increase the energy density of SIBs/KIBs. The electrochemical voltage window is directly associated with the components of PE matrices and plasticizers, the type and concentration of salt, synthesis procedure, etc. and rational design is of significance.
5. Excellent thermal stability: In addition to that PEs should be inert relative to other battery electrode components to avoid electrochemical instability and detrimental side reactions, the excellent thermal stability of PEs can ensure the safety of batteries even operated at a high-temperature environment or under some emergency circumstances of the short circuit, overcharge, etc. Introducing nonflammable components or additives is a feasible strategy to improve the thermal stability of PEs.

Last but not least, the interface issues between electrode and electrolyte are a critical topic in batteries. When the interface is in loose contact, the ion transport rate and the cycle stability of the batteries are limited. Moreover, the unstable electrode/electrolyte interfaces will allow the occurrence of side reactions and dendrites. A more in-depth discussion on the interface mechanism might be of great help to battery performance. Pointing at the development of Na^+/K^+-based quasi-/solid electrolytes, studies also should focus on environmental protection and cost reduction, and developing high safety, non-toxic, degradable and accessible materials, such as cellulose and polysaccharide.

Acknowledgements

H.Y. and C.J.H. contributed equally to this work. This work was supported by the Key-Area Research and Development Program of Guangdong Province (2019B090914003), National Natural Science Foundation of China (11904379, 51822210, 51972329), Shenzhen Science and Technology Planning Project (JCYJ20200109115624923, JCYJ20190807171803813, KQTD20161129150510559), China Postdoctoral Science Foundation (2018M643235), and Natural Science Foundation of Guangdong Province (2019A1515011902).

Conflict of Interest

The authors declare no conflict of interest.

Keywords

ionic conductivity, polymer electrolytes, potassium-ion batteries, sodium-ion batteries

Received: October 25, 2020
Revised: November 27, 2020
Published online: May 28, 2021

[1] C. Sun, J. Liu, Y. Gong, D. P. Wilkinson, J. Zhang, *Nano Energy* **2017**, *33*, 363.
[2] J. Hao, J. Zhang, G. Xia, Y. Liu, Y. Zheng, W. Zhang, Y. B. Tang, W. K. Pang, Z. Guo, *ACS Nano* **2018**, *12*, 10430.
[3] D. Lin, Y. Liu, Y. Cui, *Nat. Nanotechnol.* **2017**, *12*, 194.
[4] A. Yu, D. Gong, M. Zhang, Y. Tang, *Chem. Eng. J.* **2020**, *401*, 125834.
[5] R. Yang, F. Zhang, X. Lei, Y. Zheng, G. Zhao, Y. Tang, C.-S. Lee, *ACS Appl. Mater. Interfaces* **2020**, *12*, 47539.
[6] Y. Liu, N. Zhang, F. Wang, X. Liu, L. Jiao, L.-Z. Fan, *Adv. Funct. Mater.* **2018**, *28*, 1801917.
[7] X. Lei, Y. P. Zheng, F. Zhang, Y. Wang, Y. B. Tang, *Energy Storage Mater.* **2020**, *30*, 34.
[8] B. F. Ji, W. J. Yao, Y. B. Tang, *Sustainable Energy Fuels* **2020**, *4*, 101.
[9] K. Vignarooban, R. Kushagra, A. Elango, P. Badami, B. E. Mellander, X. Xu, T. G. Tucker, C. Nam, A. M. Kannan, *Int. J. Hydrogen Energy* **2016**, *41*, 2829.
[10] X. Deng, K. Zou, P. Cai, B. Wang, H. Hou, G. Zou, X. Ji, *Small Methods* **2020**, *4*, 2000401.
[11] T. Y. Song, W. J. Yao, P. Kiadkhunthod, Y. P. Zheng, N. Z. Wu, X. L. Zhou, S. Tunmee, S. Sattayaporn, Y. B. Tang, *Angew. Chem., Int. Ed.* **2020**, *59*, 740.
[12] J. Lang, J. Li, F. Zhang, X. Ding, J. A. Zapien, Y. Tang, *Batteries Supercaps* **2019**, *2*, 440.
[13] J. Zhang, Y. Liu, X. Zhao, L. He, H. Liu, Y. Song, S. Sun, Q. Li, X. Xing, J. Chen, *Adv. Mater.* **2020**, *32*, 1906348.
[14] G. Zhang, X. Ou, C. Cui, J. Ma, J. Yang, Y. Tang, *Adv. Funct. Mater.* **2018**, *29*, 1806722.
[15] C. Jiang, Y. Fang, W. Zhang, X. Song, J. Lang, L. Shi, Y. Tang, *Angew. Chem., Int. Ed.* **2018**, *57*, 16370.
[16] M. Sheng, F. Zhang, B. Ji, X. Tong, Y. Tang, *Adv. Energy Mater.* **2017**, *7*, 1601963.
[17] S. Mu, Q. Liu, P. Kidkhunthod, X. Zhou, W. Wang, Y. Tang, *Natl. Sci. Rev.* **2020**. https://doi.org/10.1093/nsr/nwaa178.
[18] S. Dühnen, J. Betz, M. Kolek, R. Schmuch, M. Winter, T. Placke, *Small Methods* **2020**, *4*, 2000039.
[19] X. Q. Chang, X. L. Zhou, X. W. Ou, C. S. Lee, J. W. Zhou, Y. B. Tang, *Adv. Energy Mater.* **2019**, *9*, 1902672.
[20] B. Ji, W. Yao, Y. Zheng, P. Kidkhunthod, X. Zhou, S. Tunmee, S. Sattayaporn, H.-M. Cheng, H. He, Y. Tang, *Nat. Commun.* **2020**, *11*, 1225.
[21] A. Yu, Q. Pan, M. Zhang, D. Xie, Y. Tang, *Adv. Funct. Mater.* **2020**, *30*, 2001440.
[22] H. He, W. Yao, S. Tunmee, X. Zhou, B. Ji, N. Wu, T. Song, P. Kidkhunthod, Y. Tang, *J. Mater. Chem. A* **2020**, *8*, 9128.
[23] K. Shin, Y. Zheng, F. Zhang, S. Wu, Y. Tang, *ACS Appl. Energy Mater.* **2020**, *3*, 7030.
[24] C. Zhao, L. Liu, X. Qi, Y. Lu, F. Wu, J. Zhao, Y. Yu, Y.-S. Hu, L. Chen, *Adv. Energy Mater.* **2018**, *8*, 1703012.
[25] K. Kubota, S. Komaba, *J. Electrochem. Soc.* **2015**, *162*, A2538.
[26] H. Che, S. Chen, Y. Xie, H. Wang, K. Amine, X.-Z. Liao, Z.-F. Ma, *Energy Environ. Sci.* **2017**, *10*, 1075.
[27] N. Yabuuchi, K. Kubota, M. Dahbi, S. Komaba, *Chem. Rev.* **2014**, *114*, 11636.

[28] Y. Xu, C. Zhang, M. Zhou, Q. Fu, C. Zhao, M. Wu, Y. Lei, *Nat. Commun.* **2018**, *9*, 1720.
[29] X. Wu, D. P. Leonard, X. Ji, *Chem. Mater.* **2017**, *29*, 5031.
[30] Y. Wen, K. He, Y. Zhu, F. Han, Y. Xu, I. Matsuda, Y. Ishii, J. Cumings, C. Wang, *Nat. Commun.* **2014**, *5*, 4033.
[31] W. Li, K. Wang, M. Zhou, H. Zhan, S. Cheng, K. Jiang, *ACS Appl. Mater. Interfaces* **2018**, *10*, 22059.
[32] D. Su, A. McDonagh, S. Z. Qiao, G. Wang, *Adv. Mater.* **2017**, *29*, 1604007.
[33] D. Kundu, E. Talaie, V. Duffort, L. F. Nazar, *Angew. Chem., Int. Ed.* **2015**, *54*, 3431.
[34] K. Kubota, M. Dahbi, T. Hosaka, S. Kumakura, S. Komaba, *Chem. Rev.* **2018**, *18*, 459.
[35] F. Wang, N. Zhang, X. Zhao, L. Wang, J. Zhang, T. Wang, F. Liu, Y. Liu, L.-Z. Fan, *Adv. Sci.* **2019**, *6*, 1900649.
[36] J.-Y. Hwang, S.-T. Myung, Y.-K. Sun, *Adv. Funct. Mater.* **2018**, *28*, 1802938.
[37] J. Y. Hwang, S. T. Myung, Y. K. Sun, *Chem. Soc. Rev.* **2017**, *46*, 3529.
[38] A. Eftekhari, Z. Jian, X. Ji, *ACS Appl. Mater. Interfaces* **2017**, *9*, 4404.
[39] H. Pan, Y.-S. Hu, L. Chen, *Energy Environ. Sci.* **2013**, *6*, 2338.
[40] D. Liu, L. Yang, Z. Chen, G. Zou, H. Hou, J. Hu, X. Ji, *Sci. Bull.* **2020**, *65*, 1003.
[41] Q. Shen, X. Zhao, Y. Liu, Y. Li, J. Zhang, N. Zhang, C. Yang, J. Chen, *Adv. Sci.* **2020**, *7*, 2002199.
[42] L. Yang, W. Hong, Y. Zhang, Y. Tian, X. Gao, Y. Zhu, G. Zou, H. Hou, X. Ji, *Adv. Funct. Mater.* **2019**, *29*, 1903454.
[43] A. Wang, W. Hong, L. Yang, Y. Tian, X. Qiu, G. Zou, H. Hou, X. Ji, *Small* **2020**, *16*, 2004022.
[44] X. Xu, K. Lin, D. Zhou, Q. Liu, X. Qin, S. Wang, S. He, F. Kang, B. Li, G. Wang, *Chem* **2020**, *6*, 902.
[45] N. Kumar, D. J. Siegel, *J. Phys. Chem. Lett.* **2016**, *7*, 874.
[46] J. B. Goodenough, Y. Kim, *Chem. Mater.* **2010**, *22*, 587.
[47] A. Ponrouch, R. Dedryvère, D. Monti, A. E. Demet, J. M. Ateba Mba, L. Croguennec, C. Masquelier, P. Johansson, M. R. Palacín, *Energy Environ. Sci.* **2013**, *6*, 2361.
[48] L. Zhou, Z. Cao, J. Zhang, Q. Sun, Y. Wu, W. Wahyudi, J.-Y. Hwang, L. Wang, L. Cavallo, Y.-K. Sun, H. N. Alshareef, J. Ming, *Nano Lett.* **2020**, *20*, 3247.
[49] R. Thangavel, M. Moorthy, B. K. Ganesan, W. Lee, W. S. Yoon, Y. S. Lee, *Small* **2020**, *16*, 2003688.
[50] M. Okoshi, Y. Yamada, S. Komaba, A. Yamada, H. Nakai, *J. Electrochem. Soc.* **2016**, *164*, A54.
[51] X. Zhang, Z. Wei, K. N. Dinh, N. Chen, G. Chen, F. Du, Q. Yan, *Small* **2020**, *16*, 2002700.
[52] X. Q. Zhang, X. Chen, X. B. Cheng, B. Q. Li, X. Shen, C. Yan, J. Q. Huang, Q. Zhang, *Angew. Chem., Int. Ed.* **2018**, *57*, 5301.
[53] Y. Huang, L. Zhao, L. Li, M. Xie, F. Wu, R. Chen, *Adv. Mater.* **2019**, *31*, 1808393.
[54] Y. Li, Z. Gao, F. Hu, X. Lin, Y. Wei, J. Peng, J. Yang, Z. Li, Y. Huang, H. Ding, *Small Methods* **2020**, *4*, 2000111.
[55] Z. Shen, W. Zhang, G. Zhu, Y. Huang, Q. Feng, Y. Lu, *Small Methods* **2020**, *4*, 1900592.
[56] Y. Liu, C. Gao, L. Dai, Q. Deng, L. Wang, J. Luo, S. Liu, N. Hu, *Small* **2020**, *16*, 2004096.
[57] X. Li, X. Ou, Y. Tang, *Adv. Energy Mater.* **2020**, *10*, 2002567.
[58] N. Li, F. Zhang, Y. B. Tang, *J. Mater. Chem. A* **2018**, *6*, 17889.
[59] H. Hou, C. E. Banks, M. Jing, Y. Zhang, X. Ji, *Adv. Mater.* **2015**, *27*, 7861.
[60] X. Zhang, M. Dong, Y. Xiong, Z. Hou, H. Ao, M. Liu, Y. Zhu, Y. Qian, *Small* **2020**, *16*, 2003585.
[61] S. A. Pervez, G. Kim, B. P. Vinayan, M. A. Cambaz, M. Kuenzel, M. Hekmatfar, M. Fichtner, S. Passerini, *Small* **2020**, *16*, 2000279.
[62] Y. Lu, L. Li, Q. Zhang, Z. Niu, J. Chen, *Joule* **2018**, *2*, 1747.
[63] L. Long, S. Wang, M. Xiao, Y. Meng, *J. Mater. Chem. A* **2016**, *4*, 10038.
[64] A. Manuel Stephan, K. S. Nahm, *Polymer* **2006**, *47*, 5952.
[65] P. Yao, H. Yu, Z. Ding, Y. Liu, J. Lu, M. Lavorgna, J. Wu, X. Liu, *Front. Chem.* **2019**, *7*, 522.
[66] Y. Liu, B. Xu, W. Zhang, L. Li, Y. Lin, C. Nan, *Small* **2020**, *16*, 1902813.
[67] D. E. Fenton, J. M. Parker, P. V. Wright, *Polymer* **1973**, *14*, 589.
[68] H. Fei, Y. Liu, Y. An, X. Xu, J. Zhang, B. Xi, S. Xiong, J. Feng, *J. Power Sources* **2019**, *433*, 226697.
[69] S. Choudhury, S. Wei, Y. Ozhabes, D. Gunceler, M. J. Zachman, Z. Tu, J. H. Shin, P. Nath, A. Agrawal, L. F. Kourkoutis, T. A. Arias, L. A. Archer, *Nat. Commun.* **2017**, *8*, 898.
[70] G. Åvall, J. Mindemark, D. Brandell, P. Johansson, *Adv. Energy Mater.* **2018**, *8*, 1703036.
[71] J. Chai, Z. Liu, J. Ma, J. Wang, X. Liu, H. Liu, J. Zhang, G. Cui, L. Chen, *Adv. Sci.* **2017**, *4*, 1600377.
[72] X. Yu, A. Manthiram, *Energy Environ. Sci.* **2018**, *11*, 527.
[73] S. Wang, Y. Chen, Y. Jie, S. Lang, J. Song, Z. Lei, S. Wang, X. Ren, D. Wang, X. Li, R. Cao, G. Zhang, S. Jiao, *Small Methods* **2020**, *4*, 1900856.
[74] L. Xiang, X. Ou, X. Wang, Z. Zhou, X. Li, Y. Tang, *Angew. Chem., Int. Ed.* **2020**, *59*, 17924.
[75] X. Zhou, Q. Liu, C. Jiang, B. Ji, X. Ji, Y. Tang, H. M. Cheng, *Angew. Chem., Int. Ed.* **2020**, *59*, 3802.
[76] C. Jiang, L. Xiang, S. Miao, L. Shi, D. Xie, J. Yan, Z. Zheng, X. Zhang, Y. Tang, *Adv. Mater.* **2020**, *32*, 1908470.
[77] Q. Liu, H. Wang, C. Jiang, Y. Tang, *Energy Storage Mater.* **2019**, *23*, 566.
[78] L. Suo, O. Borodin, W. Sun, X. Fan, C. Yang, F. Wang, T. Gao, Z. Ma, M. Schroeder, A. von Cresce, S. M. Russell, M. Armand, A. Angell, K. Xu, C. Wang, *Angew. Chem., Int. Ed.* **2016**, *55*, 7136.
[79] A. Eftekhari, *Adv. Energy Mater.* **2018**, *8*, 1801156.
[80] X. Yu, W. A. Yu, A. Manthiram, *Small Methods* **2020**, *4*, 1900697.
[81] D. Lei, Y. B. He, H. Huang, Y. Yuan, G. Zhong, Q. Zhao, X. Hao, D. Zhang, C. Lai, S. Zhang, J. Ma, Y. Wei, Q. Yu, W. Lv, Y. Yu, B. Li, Q. H. Yang, Y. Yang, J. Lu, F. Kang, *Nat. Commun.* **2019**, *10*, 4244.
[82] J. Yang, H. Zhang, Q. Zhou, H. Qu, T. Dong, M. Zhang, B. Tang, J. Zhang, G. Cui, *ACS Appl. Mater. Interfaces* **2019**, *11*, 17109.
[83] L. Fan, S. Wei, S. Li, Q. Li, Y. Lu, *Adv. Energy Mater.* **2018**, *8*, 1702657.
[84] J. Yu, S. Duan, B. Huang, H. Jin, S. Xie, J. Li, *Small Methods* **2020**, *4*, 2000308.
[85] A. Banerjee, K. H. Park, J. W. Heo, Y. J. Nam, C. K. Moon, S. M. Oh, S. T. Hong, Y. S. Jung, *Angew. Chem., Int. Ed.* **2016**, *55*, 9634.
[86] A. Hayashi, K. Noi, A. Sakuda, M. Tatsumisago, *Nat. Commun.* **2012**, *3*, 856.
[87] Z. Zhang, Q. Zhang, C. Ren, F. Luo, Q. Ma, Y.-S. Hu, Z. Zhou, H. Li, X. Huang, L. Chen, *J. Mater. Chem. A* **2016**, *4*, 15823.
[88] S. Li, S. Q. Zhang, L. Shen, Q. Liu, J. B. Ma, W. Lv, Y. B. He, Q. H. Yang, *Adv. Sci.* **2020**, *7*, 1903088.
[89] C. Sångeland, R. Younesi, J. Mindemark, D. Brandell, *Energy Storage Mater.* **2019**, *19*, 31.
[90] H. Ao, Y. Zhao, J. Zhou, W. Cai, X. Zhang, Y. Zhu, Y. Qian, *J. Mater. Chem. A* **2019**, *7*, 18708.
[91] F. Baskoro, H. Q. Wong, H.-J. Yen, *ACS Appl. Energy Mater.* **2019**, *2*, 3937.
[92] T. T. Beyene, H. K. Bezabh, M. A. Weret, T. M. Hagos, C.-J. Huang, C.-H. Wang, W.-N. Su, H. Dai, B.-J. Hwang, *J. Electrochem. Soc.* **2019**, *166*, A1501.
[93] X. Cheng, J. Pan, Y. Zhao, M. Liao, H. Peng, *Adv. Energy Mater.* **2018**, *8*, 1702184.
[94] Q. Wang, H. Zhang, Z. Cui, Q. Zhou, X. Shangguan, S. Tian, X. Zhou, G. Cui, *Energy Storage Mater.* **2019**, *23*, 466.
[95] K. Yoshida, M. Nakamura, Y. Kazue, N. Tachikawa, S. Tsuzuki, S. Seki, K. Dokko, M. Watanabe, *J. Am. Chem. Soc.* **2011**, *133*, 13121.

[96] S. Janakiraman, O. Padmaraj, S. Ghosh, A. Venimadhav, *J. Electroanal. Chem.* **2018**, *826*, 142.
[97] J. Manuel, X. Zhao, K.-K. Cho, J.-K. Kim, J.-H. Ahn, *ACS Sustainable Chem. Eng.* **2018**, *6*, 8159.
[98] M. Jahn, M. Sedlarikova, J. Vondrak, L. Palizek, *ECS Trans.* **2016**, *74*, 159.
[99] W.-T. Whang, L.-H. Yanc, Y.-W. Fan, *J. Appl. Polym. Sci.* **1994**, *54*, 923.
[100] Y. L. Ni'mah, M.-Y. Cheng, J. H. Cheng, J. Rick, B.-J. Hwang, *J. Power Sources* **2015**, *278*, 375.
[101] K. Kiran Kumar, M. Ravi, Y. Pavani, S. Bhavani, A. K. Sharma, V. V. R. Narasimha Rao, *Phys. B* **2011**, *406*, 1706.
[102] K. S. Ngai, S. Ramesh, K. Ramesh, J. C. Juan, *Ionics* **2016**, *22*, 1259.
[103] A. Bhide, K. Hariharan, *Polym. Int.* **2008**, *57*, 523.
[104] A. Chandra, A. Chandra, K. Thakur, *Arabian J. Chem.* **2016**, *9*, 400.
[105] F. Croce, G. B. Appetecchi, L. Persi, B. Scrosati, *Nature* **1998**, *394*, 456.
[106] A. Dey, T. Ghoshal, S. Karan, S. K. De, *J. Appl. Phys.* **2011**, *110*, 043707.
[107] Y. W. S. H. Chunga, L. Persi, F. Croce, S. G. Greenbaum, B. Scrosati, E. Plichta, *J. Power Sources* **2001**, *97-98*, 644.
[108] S. Song, M. Kotobuki, F. Zheng, C. Xu, S. V. Savilov, N. Hu, L. Lu, Y. Wang, W. D. Z. Li, *J. Mater. Chem. A* **2017**, *5*, 6424.
[109] I. Villaluenga, X. Bogle, S. Greenbaum, I. Gil de Muro, T. Rojo, M. Armand, *J. Mater. Chem. A* **2013**, *1*, 8348.
[110] H. Zhang, J. Wang, X. Xuan, K. Zhuo, *Electrochim. Acta* **2006**, *51*, 3244.
[111] A. Arya, N. G. Saykar, A. L. Sharma, *J. Appl. Polym. Sci.* **2019**, *136*, 47361.
[112] Q. Zhou, B. Xu, P.-H. Chien, Y. Li, B. Huang, N. Wu, H. Xu, N. S. Grundish, Y.-Y. Hu, J. B. Goodenough, *Small Methods* **2020**, *4*, 2000764.
[113] X. Yu, L. Xue, J. B. Goodenough, A. Manthiram, *ACS Mater. Lett.* **2019**, *1*, 132.
[114] C. Ma, K. Dai, H. Hou, X. Ji, L. Chen, D. G. Ivey, W. Wei, *Adv. Sci.* **2018**, *5*, 1700996.
[115] K. K. Kumar, M. Ravi, Y. Pavani, S. Bhavani, A. K. Sharma, V. V. R. Narasimha Rao, *J. Membr. Sci.* **2014**, *454*, 200.
[116] H. K. Koduru, L. Marino, F. Scarpelli, A. G. Petrov, Y. G. Marinov, G. B. Hadjichristov, M. T. Iliev, N. Scaramuzza, *Curr. Appl. Phys.* **2017**, *17*, 1518.
[117] A. Arya, A. L. Sharma, *J. Solid State Electrochem.* **2018**, *22*, 2725.
[118] A. A. Pritam, A. L. Sharma, *J. Mater. Sci.* **2019**, *54*, 7131.
[119] J.-H. Shin, S. Passerini, *Electrochim. Acta* **2004**, *49*, 1605.
[120] N. Lago, O. Garcia-Calvo, J. M. Lopez del Amo, T. Rojo, M. Armand, *ChemSusChem* **2015**, *8*, 3039.
[121] H. B. Youcef, B. Orayech, J. M. L. Del Amo, F. Bonilla, D. Shanmukaraj, M. Armand, *Solid State Ionics* **2020**, *345*, 115168.
[122] J. Serra Moreno, M. Armand, M. B. Berman, S. G. Greenbaum, B. Scrosati, S. Panero, *J. Power Sources* **2014**, *248*, 695.
[123] Q. Ma, J. Liu, X. Qi, X. Rong, Y. Shao, W. Feng, J. Nie, Y.-S. Hu, H. Li, X. Huang, L. Chen, Z. Zhou, *J. Mater. Chem. A* **2017**, *5*, 7738.
[124] C. Zhao, L. Liu, Y. Lu, M. Wagemaker, L. Chen, Y. S. Hu, *Angew. Chem., Int. Ed.* **2019**, *58*, 17026.
[125] Z. Zhu, R. Kan, S. Hu, L. He, X. Hong, H. Tang, W. Luo, *Small* **2020**, *16*, 2003251.
[126] X. Qi, Q. Ma, L. Liu, Y.-S. Hu, H. Li, Z. Zhou, X. Huang, L. Chen, *ChemElectroChem* **2016**, *3*, 1741.
[127] G. Du, M. Tao, J. Li, T. Yang, W. Gao, J. Deng, Y. Qi, S. J. Bao, M. Xu, *Adv. Energy Mater.* **2020**, *10*, 1903351.
[128] J. Mindemark, B. Sun, E. Törmä, D. Brandell, *J. Power Sources* **2015**, *298*, 166.
[129] Y. Yao, Z. Wei, H. Wang, H. Huang, Y. Jiang, X. Wu, X. Yao, Z. S. Wu, Y. Yu, *Adv. Energy Mater.* **2020**, *10*, 1903698.
[130] Z. Wei, S. Chen, J. Wang, Z. Wang, Z. Zhang, X. Yao, Y. Deng, X. Xu, *J. Mater. Chem. A* **2018**, *6*, 13438.
[131] G. Feuillade, P. Perche, *J. Appl. Electrochem.* **1975**, *5*, 63.
[132] J. Shi, H. Xiong, Y. Yang, H. Shao, *Solid State Ionics* **2018**, *326*, 136.
[133] Y.-S. Lee, J. H. Lee, J.-A. Choi, W. Y. Yoon, D.-W. Kim, *Adv. Funct. Mater.* **2013**, *23*, 1019.
[134] J. Hassoun, P. Reale, B. Scrosati, *J. Mater. Chem.* **2007**, *17*, 3668.
[135] L. Zhou, N. Wu, Q. Cao, B. Jing, X. Wang, Q. Wang, H. Kuang, *Solid State Ionics* **2013**, *249-250*, 93.
[136] A. Subramania, N. T. K. Sundaram, G. V. Kumar, *J. Power Sources* **2006**, *153*, 177.
[137] L. Balo, H. G. Shalu, V. Kumar Singh, R. Kumar Singh, *Electrochim. Acta* **2017**, *230*, 123.
[138] T. Ma, Z. Cui, Y. Wu, S. Qin, H. Wang, F. Yan, N. Han, J. Li, *J. Membr. Sci.* **2013**, *444*, 213.
[139] Y.-W. Lee, W.-K. Shin, D.-W. Kim, *Solid State Ionics* **2014**, *255*, 6.
[140] J.-A. Choi, Y. Kang, H. Shim, D. W. Kim, E. Cha, D.-W. Kim, *J. Power Sources* **2010**, *195*, 6177.
[141] F. Colò, F. Bella, J. R. Nair, C. Gerbaldi, *J. Power Sources* **2017**, *365*, 293.
[142] M. L. Lehmann, G. Yang, D. Gilmer, K. S. Han, E. C. Self, R. E. Ruther, S. Ge, B. Li, V. Murugesan, A. P. Sokolov, F. M. Delnick, J. Nanda, T. Saito, *Energy Storage Mater.* **2019**, *21*, 85.
[143] V. Aravindan, P. Vickraman, A. Sivashanmugam, R. Thirunakaran, S. Gopukumar, *Curr. Appl. Phys.* **2013**, *13*, 293.
[144] W. K. Shin, J. Cho, A. G. Kannan, Y. S. Lee, D. W. Kim, *Sci. Rep.* **2016**, *6*, 26332.
[145] T. Umecky, Y. Saito, Y. Okumura, S. Maeda, T. Sakai, *J. Phys. Chem. B* **2008**, *112*, 3357.
[146] Q. Yang, Z. Zhang, X. G. Sun, Y. S. Hu, H. Xing, S. Dai, *Chem. Soc. Rev.* **2018**, *47*, 2020.
[147] M. Xie, S. Li, Y. Huang, Z. Wang, Y. Jiang, M. Wang, F. Wu, R. Chen, *ChemElectroChem* **2019**, *6*, 2423.
[148] K. Matsumoto, S. Sogabe, T. Endo, *J. Polym. Sci., Part A: Polym. Chem.* **2012**, *50*, 1317.
[149] J.-H. Shin, W. A. Henderson, C. Tizzani, S. Passerini, S.-S. Jeong, K.-W. Kim, *J. Electrochem. Soc.* **2006**, *153*, A1649.
[150] G. Chen, Y. Bai, Y. Gao, Z. Wang, K. Zhang, Q. Ni, F. Wu, H. Xu, C. Wu, *ACS Appl. Mater. Interfaces* **2019**, *11*, 43252.
[151] A. Boschin, P. Johansson, *Electrochim. Acta* **2016**, *211*, 1006.
[152] J.-H. Shin, W. A. Henderson, S. Passerini, *ECS Solid State Lett.* **2005**, *8*, A125.
[153] Y. Zhu, F. Wang, L. Liu, S. Xiao, Z. Chang, Y. Wu, *Energy Environ. Sci.* **2013**, *6*, 618.
[154] M. Waqas, C. Tan, W. Lv, S. Ali, B. Boateng, W. Chen, Z. Wei, C. Feng, J. Ahmed, J. B. Goodenough, W. He, *ChemElectroChem* **2018**, *5*, 2722.
[155] S. Janakiraman, A. Surendran, S. Ghosh, S. Anandhan, A. Venimadhav, *Solid State Ionics* **2016**, *292*, 130.
[156] S. Janakiraman, A. Surendran, R. Biswal, S. Ghosh, S. Anandhan, A. Venimadhav, *Mater. Res. Express* **2019**, *6*, 086318.
[157] P. C. W. A. Du Pasquier, D. Culver, A. S. Gozdz, G. G. Amatucci, J.-M. Tarasconb, *Solid State Ionics* **2000**, *135*, 249.
[158] F. Wang, X. Wang, Z. Chang, X. Wu, X. Liu, L. Fu, Y. Zhu, Y. Wu, W. Huang, *Adv. Mater.* **2015**, *27*, 6962.
[159] Y. Zhu, Y. Yang, L. Fu, Y. Wu, *Electrochim. Acta* **2017**, *224*, 405.
[160] Y. Zhu, F. Wang, L. Liu, S. Xiao, Y. Yang, Y. Wu, *Sci. Rep.* **2013**, *3*, 3187.
[161] J. I. Kim, K. Y. Chung, J. H. Park, *J. Membr. Sci.* **2018**, *566*, 122.
[162] J. I. Kim, Y. Choi, K. Y. Chung, J. H. Park, *Adv. Funct. Mater.* **2017**, *27*, 1701768.
[163] H. Gao, B. Guo, J. Song, K. Park, J. B. Goodenough, *Adv. Energy Mater.* **2015**, *5*, 1402235.
[164] D. Xie, M. Zhang, Y. Wu, L. Xiang, Y. Tang, *Adv. Funct. Mater.* **2019**, *30*, 1906770.

[165] K. Mishra, T. Arif, R. Kumar, D. Kumar, *J. Solid State Electrochem.* **2019**, *23*, 2401.
[166] Y. Xue, D. J. Quesnel, *RSC Adv.* **2016**, *6*, 7504.
[167] K. Vignarooban, P. Badami, M. A. K. L. Dissanayake, P. Ravirajan, A. M. Kannan, *Ionics* **2017**, *23*, 2817.
[168] C. Venkata Subba Rao, M. Ravi, V. Raja, P. Balaji Bhargav, A. K. Sharma, V. V. R. Narasimha Rao, *Iran. Polym. J.* **2012**, *21*, 531.
[169] C. V. Subba Reddy, A. P. Jin, Q. Y. Zhu, L. Q. Mai, W. Chen, *Eur. Phys. J. E* **2006**, *19*, 471.
[170] Z. Osman, K. B. Md Isa, A. Ahmad, L. Othman, *Ionics* **2010**, *16*, 431.
[171] N. K. Jyothi, K. V. Kumar, G. S. Sundari, P. N. Murthy, *Indian J. Phys.* **2015**, *90*, 289.
[172] R. Sathiyamoorthi, R. Chandrasekaran, S. Selladurai, T. Vasudevan, *Ionics* **2003**, *9*, 404.
[173] Y. Xue, *Int. J. Electrochem. Sci.* **2017**, *12*, 10674.
[174] D. Kumar, S. A. Hashmi, *J. Power Sources* **2010**, *195*, 5101.
[175] M. C. Rao, R. Koutavarapu, K. V. Kumar, *Mater. Sci. Semicond. Process.* **2019**, *89*, 41.
[176] B. Chandni, S. Ram, A. Anil, A. L. Sharma, *Mater. Sci. Eng., B* **2015**, *5*, 418.
[177] M. Rao, X. Geng, Y. Liao, S. Hu, W. Li, *J. Membr. Sci.* **2012**, *399-400*, 37.
[178] C. Zhang, Y. Xu, K. He, Y. Dong, H. Zhao, L. Medenbach, Y. Wu, A. Balducci, T. Hannappel, Y. Lei, *Small* **2020**, *16*, 2002953.
[179] H. Gao, L. Xue, S. Xin, J. B. Goodenough, *Angew. Chem., Int. Ed.* **2018**, *57*, 5449.
[180] X. Yuan, B. Zhu, J. Feng, C. Wang, X. Cai, K. Qiao, R. Qin, *Small* **2020**, *16*, 2003386.
[181] Y. Pavani, M. Ravi, S. Bhavani, R. S. Karthikeya, V. V. R. N. Rao, *J. Mater. Sci.: Mater. Electron.* **2018**, *29*, 5518.
[182] R. Singh, J. Baghel, S. Shukla, B. Bhattacharya, H.-W. Rhee, P. K. Singh, *Phase Transitions* **2014**, *87*, 1237.
[183] A. Chandra, *Indian J. Phys.* **2015**, *90*, 759.
[184] Y. Pavani, M. Ravi, S. Bhavani, A. K. Sharma, V. V. R. Narasimha Rao, *Polym. Eng. Sci.* **2012**, *52*, 1685.
[185] P. Kesharwani, D. K. Sahu, M. Sahu, T.b. Sahu, R. C. Agrawal, *Ionics* **2016**, *23*, 2823.
[186] J. Siva Kumar, M. Jaipal Reddy, U. V. Subba Rao, *J. Mater. Sci.* **2006**, *41*, 6171.
[187] M. Rayung, M. M. Aung, A. Ahmad, M. S. Su'ait, L. C. Abdullah, S. N. Ain Md Jamil, *Mater. Chem. Phys.* **2019**, *222*, 110.
[188] J. Zhang, J. Yang, T. Dong, M. Zhang, J. Chai, S. Dong, T. Wu, X. Zhou, G. Cui, *Small* **2018**, *14*, 1800821.
[189] J. Zhang, J. Zhao, L. Yue, Q. Wang, J. Chai, Z. Liu, X. Zhou, H. Li, Y. Guo, G. Cui, L. Chen, *Adv. Energy Mater.* **2015**, *5*, 1501082.
[190] M. S. Su'ait, A. Ahmad, K. H. Badri, N. S. Mohamed, M. Y. A. Rahman, C. L. A. Ricardo, P. Scardi, *Int. J. Hydrogen Energy* **2014**, *39*, 3005.
[191] H. Fei, Y. Liu, Y. An, X. Xu, G. Zeng, Y. Tian, L. Ci, B. Xi, S. Xiong, J. Feng, *J. Power Sources* **2018**, *399*, 294.
[192] C. V. Subba Reddy, A. K. Sharma, V. V. R. Narasimha Rao, *J. Power Sources* **2003**, *114*, 338.
[193] B. A. Sarada, P. B. Bhargav, A. K. Sharma, V. V. R. N. Rao, *Mater. Res. Innovations* **2013**, *15*, 394.
[194] N. Reddeppa, A. K. Sharma, V. V. R. Narasimha Rao, W. Chen, *Measurement* **2014**, *47*, 33.
[195] R. Nadimicherla, A. K. Sharma, V. V. R. N. Rao, W. Chen, *Ionics* **2014**, *21*, 1587.
[196] K. J. Lee, J. T. Park, J. H. Koh, B. R. Min, J. H. Kim, *Ionics* **2008**, *15*, 163.
[197] P. Kesharwani, D. K. Sahu, Y. K. Mahipal, R. C. Agrawal, *Mater. Chem. Phys.* **2017**, *193*, 524.
[198] A. Chandra, *Compos. Commun.* **2017**, *4*, 33.
[199] A. Dey, S. Karan, A. Dey, S. K. De, *Mater. Res. Bull.* **2011**, *46*, 2009.
[200] N. K. Jyothi, K. K. Venkataratnam, P. N. Murty, K. V. Kumar, *Bull. Mater. Sci.* **2016**, *39*, 1047.
[201] F. Lv, Z. Wang, L. Shi, J. Zhu, K. Edström, J. Mindemark, S. Yuan, *J. Power Sources* **2019**, *441*, 227175.
[202] Y. Li, X. Chen, A. Dolocan, Z. Cui, S. Xin, L. Xue, H. Xu, K. Park, J. B. Goodenough, *J. Am. Chem. Soc.* **2018**, *140*, 6448.
[203] J. Lang, J. Li, X. Ou, F. Zhang, K. Shin, Y. Tang, *ACS Appl. Mater. Interfaces* **2020**, *12*, 2424.
[204] K. Deng, Q. Zeng, D. Wang, Z. Liu, Z. Qiu, Y. Zhang, M. Xiao, Y. Meng, *J. Mater. Chem. A* **2020**, *8*, 1557.
[205] B. Commarieu, A. Paolella, J.-C. Daigle, K. Zaghib, *Curr. Opin. Electrochem.* **2018**, *9*, 56.

Hang Yin is a graduate student at University of Science and Technology LiaoNing, majoring in materials science and engineering. He is currently a guest student in the Functional Thin Films Research Center, SIAT, CAS. His research focuses on the exploration of electrolytes and solid-liquid interfacial modification.

Chengjun Han is a graduate student at Nano Science and Technology Institute of University of Science and Technology of China (USTC), majoring in materials science and engineering. He is currently a guest student in the Functional Thin Films Research Center, SIAT, CAS. His research focuses on the exploration of polymer electrolytes and secondary battery electrolytes.

Qirong Liu is currently a research assistant at Functional Thin Films Research Centre, Shenzhen Institutes of Advanced Technology (SIAT), Chinese Academy of Sciences. He completed his Ph.D. from Beihang University and Université Libre de Bruxelles in 2018. His research interest covers solid-state electrolytes, secondary batteries, functional thin-film materials and devices.

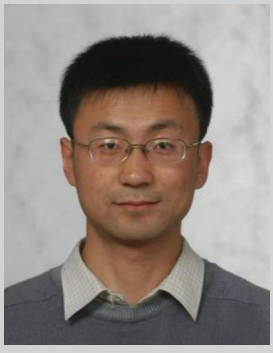

Fayu Wu received his Ph.D. from the Institute of Metal Research (IMR), Chinese Academy of Sciences (CAS) in 2006, studying microstructures, electrical and thermal transport properties, applications in Li-ion cell and supercapacitor of novel carbon materials. Currently, he works in University of Science and Technology Liaoning, and devotes himself to the exploration on preparation, characterization, and applications of 2D materials with the tailorable electrical, thermal, optical, mechanical and gas-sensing properties.

Fan Zhang is currently an associate professor at Functional Thin Films Research Centre, Shenzhen Institutes of Advanced Technology (SIAT), Chinese Academy of Sciences. She received her Ph.D. from Nankai University in 2014. Her research interest includes synthesis and applications of materials for electrochemical energy storage devices such as lithium-ion batteries, sodium-ion batteries, potassium-ion batteries, dual-ion batteries, supercapacitors.

Yongbing Tang is a doctor, professor, and director of Functional Thin Films Research Center, SIAT, CAS. He has initiated the construction of new dual-ion battery systems based on the integrated design of alloy-type anode and current collector, and further developed other novel dual-ion battery systems based on other metal ions such as Na^+, K^+, Ca^{2+}, Zn^{2+} and Mg^{2+}, opening up a new way for the development of novel energy storage devices. His research interests cover novel energy storage devices and key materials.